MARTIN MARIETTA ENERGY SYSTEMS LIBRARIES

3 4456 0333732 4

ORNL/TM-11342

ornl

OAK RIDGE NATIONAL LABORATORY

MARTIN MARIETTA

Baltimore Aircoil Company (BAC) Ice Storage Test Report

Therese K. Stovall

OAK RIDGE NATIONAL LABORATORY
CENTRAL RESEARCH LIBRARY
CIRCULATION SECTION
4500N ROOM 175
LIBRARY LOAN COPY
DO NOT TRANSFER TO ANOTHER PERSON
If you wish someone else to see this report, send in name with report and the library will arrange a loan.

MANAGED BY
MARTIN MARIETTA ENERGY SYSTEMS, INC.
FOR THE UNITED STATES
DEPARTMENT OF ENERGY

This report has been reproduced directly from the best available copy.

Available to DOE and DOE contractors from the Office of Scientific and Technical Information, P.O. Box 62, Oak Ridge, TN 37831; prices available from (615) 576-8401, FTS 626-8401.

Available to the public from the National Technical Information Service, U.S. Department of Commerce, 5285 Port Royal Rd., Springfield, VA 22161.

This report was prepared as an account of work sponsored by an agency of the United States Government. Neither the United States Government nor any agency thereof, nor any of their employees, makes any warranty, express or implied, or assumes any legal liability or responsibility for the accuracy, completeness, or usefulness of any information, apparatus, product, or process disclosed, or represents that its use would not infringe privately owned rights. Reference herein to any specific commercial product, process, or service by trade name, trademark, manufacturer, or otherwise, does not necessarily constitute or imply its endorsement, recommendation, or favoring by the United States Government or any agency thereof. The views and opinions of authors expressed herein do not necessarily state or reflect those of the United States Government or any agency thereof.

ORNL/TM-11342
Dist. Category UC-202

Engineering Technology Division

BALTIMORE AIRCOIL COMPANY (BAC) ICE STORAGE TEST REPORT

Therese K. Stovall

DATE PUBLISHED: March 1991

Prepared for the
Electric Power Research Institute
under Interagency Agreement No. DOE ERD-85-502

Prepared by the
OAK RIDGE NATIONAL LABORATORY
Oak Ridge, Tennessee 37831-6285
managed by
MARTIN MARIETTA ENERGY SYSTEMS, INC.
for the
U.S. DEPARTMENT OF ENERGY
under contract DE-AC05-840R21400

MARTIN MARIETTA ENERGY SYSTEMS LIBRARIES

3 4456 0333732 4

CONTENTS

	Page
LIST OF FIGURES	v
LIST OF TABLES	ix
ABBREVIATIONS AND SYMBOLS	xi
ACKNOWLEDGMENTS	xiii
ABSTRACT	1
1. INTRODUCTION	1
2. SYSTEMS DESCRIPTION	3
2.1BAC STORAGE SYSTEM	3
2.2 TEST FACILITY	4
3. SYSTEM TESTS	9
4. ANALYSIS METHODOLOGY	14
4.1 DATA PROCESSING	14
4.2 REFRIGERATION EFFECT	15
4.2.1 Liquid-Overfeed Coils	15
4.2.2 Brine Coils	15
4.2.3 Refrigeration System	20
4.2.4 Capacity Models and Capacity Normalization	21
4.3 DISCHARGE ENERGY AVAILABLE	22
4.4 SHELL AND AGITATION HEAT GAINS	24
5. RESULTS	25
5.1 CHARGING PERFORMANCE	25
5.1.1 Liquid-Overfeed Coils	25
5.1.2 Brine Coils	34
5.2 DISCHARGE PERFORMANCE	42
5.3 STANDBY HEAT GAINS	49
6. CONCLUSIONS AND RECOMMENDATIONS	52
REFERENCES	53
APPENDIX A. ISTF INSTRUMENTATION	55
APPENDIX B. BAC COMPUTER SIMULATION	59

LIST OF FIGURES

Figure		Page
1	ISTF schematic for BAC liquid-overfeed system	4
2	ISTF schematic for BAC brine system	5
3	Summary of corrected capacity profiles for BAC liquid-overfeed system tests	26
4	Capacity of liquid-overfeed charge tests, extended using test-specific mathematical models of capacity as function of tank charge, normalized relative to average for each test	27
5	Capacity of liquid-overfeed charge tests, generated by test-specific mathematical models of capacity as function of tank charge, normalized relative to average for each test	28
6	Suction temperature profile summary for all liquid-overfeed charging tests	30
7	Cumulative corrected capacity summary for all liquid-overfeed charging tests	30
8	Average evaporator temperature vs ice build time for BAC liquid-overfeed coils	31
9	Corrected capacity vs saturated suction temperature for tank charges from 10 to 100% frozen for BAC liquid-overfeed coils	32
10	Comparison of refrigerant temperature leaving liquid-overfeed coils to saturated temperature corresponding to refrigerant pressure at ice tank exit	33
11	Liquid-overfeed ratio summary for all liquid-overfeed charging tests	34
12	Summary of BAC brine-coil tests, capacity based on brine temperature and flow measurements, corrected according to change in tank water depth	35
13	Capacity of brine-coil charge tests, normalized relative to average for each test	36

14 Capacity of brine-coil charge tests, generated by test-specific mathematical models of capacity as function of tank charge, normalized relative to average for each test 37

15 Summary of tank brine inlet temperature profiles for all brine-coil charge tests 38

16 Summary of cumulative energy storage in ice tank for BAC brine-coil tests 38

17 Time-weighted average brine temperatures vs ice build time for BAC brine coils 39

18 Corrected capacity vs storage tank brine inlet temperature for tank charges from 10 to 100% frozen for BAC brine coils at a brine flow rate of 135 gal/min 40

19 Corrected capacity vs storage tank brine inlet temperature for tank charges from 10 to 100% frozen for BAC brine coils at a brine flow rate of 75 gal/min 41

20 Comparison of discharge energy as measured at four different locations from test run on May 24, 1989 42

21 Corrected discharge energy vs latent state of charge, or ice inventory, as measured by the tank water depth 43

22 Cumulative corrected discharge energy summary for all BAC discharge tests, ending when water temperature leaving ice tank exceeds 44°F (horizontal reference line at rated tank capacity of 266 ton-h) 44

23 BAC discharge test summary: tank water outlet temperature vs corrected cumulative discharge energy, reference line at 266 ton-h 45

24 BAC discharge test summary: tank water outlet temperature vs tank state-of-charge 46

25 BAC discharge test summary: cumulative discharge energy available for maximum tank outlet temperatures of 36, 40, 44, and 48°F for different discharge periods 47

26 Average pump power required for BAC discharge tests 48

27 BAC discharge tests at conditions beyond normal operating range: tank water outlet temperature vs time 49

28 BAC discharge tests at conditions beyond normal operating range: tank water outlet temperature vs corrected cumulative discharge energy, reference line at 266 ton-h 50

29 BAC discharge tests at conditions beyond normal operating range: tank water outlet temperature vs tank latent state of charge 50

30 Cumulative corrected discharge energy summary for BAC discharge tests at conditions beyond normal operating range 51

B.1 Comparison of test data to BAC computer model predictions for liquid-overfeed test of 0801 61

B.2 Comparison of test data to BAC computer model predictions for liquid-overfeed test of 0811 61

B.3 Comparison of test data to BAC computer model predictions for liquid-overfeed test of 0815 62

B.4 Comparison of test data to BAC computer model predictions for liquid-overfeed test of 0914 62

B.5 Comparison of test data to BAC computer model predictions for liquid-overfeed test of 0922 63

B.6 Comparison of test data to BAC computer model predictions for brine-coil test of 0523 63

B.7 Comparison of test data to BAC computer model predictions for brine-coil test of 0613 64

B.8 Comparison of test data to BAC computer model predictions for brine-coil test of 0619 64

B.9 Comparison of test data to BAC computer model predictions for brine-coil test of 0623 65

B.10 Comparison of test data to BAC computer model predictions for brine-coil test of 0628 65

B.11 Comparison of test data to BAC computer model predictions for brine-coil test of 0727 66

B.12 Comparison of test data to BAC computer model predictions for brine-coil test of 0731 66

B.13 Comparison of test data to BAC computer model predictions for brine-coil test of 0803 67

LIST OF TABLES

Table		Page
1	ISTF monitoring points for the liquid-overfeed system	6
2	ISTF monitoring points for the brine-coil system	7
3	Planned charge test sequence	10
4	Planned discharge test sequence	10
5	Planned standby test sequence	10
6	BAC charge test sequence	12
7	BAC discharge test sequence	13
A.1	Flowmeter/RTD comparative closure summary	57
B.1	BAC computer simulation liquid-overfeed coil temperatures	60
B.2	BAC computer simulation brine-coil temperature	60

ABBREVIATIONS AND SYMBOLS

BAC	Baltimore Aircoil Company
Bhp	boiler horsepower
DX	direct expansion
FE1	refrigerant flow from the condenser
FE6	water flow rate
HE1	refrigerant enthalpy entering the condenser
HE2	refrigerant enthalpy leaving the condenser
h_{fg}	enthalpy of evaporation at the refrigerant pressure measured at the ice tank outlet
ISTF	Ice Storage Test Facility
LOR	liquid-overfeed ratio
P	oil fraction refrigerant flow to the ice tank, assumed value of 0.05
PUC	public utilities commission
$\dot{Q}_f$	heat rejected by the refrigerant
$\dot{Q}_w$	heat absorbed by the cooling water
Re_f	refrigeration effect as determined by measured refrigerant flow rates and thermodynamic properties
Re_c	refrigeration capacity predicted by the capacity curves, tons
$\overline{Re}_f$	capacity measurement based on refrigerant measurement, averaged over the test period
Re_f^*	corrected capacity measurement
$\overline{Re}_w$	capacity measurement based on water depth change, averaged over the test period
RTD	resistance temperature detector
SAS	SAS Institute, Inc.
SCR	semiconductor controlled rectifier
TE19	water temperature exiting the condenser
TE20	water temperature into the condenser
T_d	saturated discharge temperature, °F
ton-h	ton-hour
T_s	saturated suction temperature, °F

W_c	compressor power predicted by the manufacturer's data, BHP
X_3	quality of refrigerant after the expansion valve
X_9	refrigerant quality at the ice tank exit

ACKNOWLEDGMENTS

This important research has been made possible by the support of the Electric Power Research Institute. I would like to thank the program manager, Ronald Wendland, for his critical support and enthusiasm. Baltimore Aircoil Company (BAC) provided the unit for testing, and Tom Carter of BAC was most helpful. John Tomlinson of Oak Ridge National Laboratory designed the Ice Storage Test Facility, supervised its construction, and has provided valuable guidance during the testing process. Delmar Fraysier is the chief operator of the test facility and made important contributions to the test procedures.

BALTIMORE AIRCOIL COMPANY (BAC) ICE STORAGE TEST REPORT*

Therese K. Stovall

ABSTRACT

The Ice Storage Test Facility (ISTF) is designed to test commercial ice storage systems. Baltimore Aircoil Company (BAC) provided a storage tank equipped with coils designed for use with a liquid overfeed refrigeration system. Separate coils were also supplied for use with a secondary fluid system. The BAC ice storage system was tested over a wide range of operating conditions. System performance was satisfactory under both charging and discharging conditions. During the liquid-overfeed ice build cycle, the evaporator temperature closely matched the manufacturer's literature. The measured average brine temperatures were slightly higher than those given in the BAC literature (i.e., the BAC report is conservative). During discharge cycles, the storage tank outlet temperature remains nearly constant below 35°F, rising only after most of the ice has been melted. The discharge performance was relatively unaffected by discharge rates or tank inlet temperatures. Based on these tests, a storage tank sized solely according to the latent ice storage capacity is capable of providing a relatively constant temperature to the load throughout most of the discharge cycle. This report describes BAC system performance fully under both charging and discharging conditions. Companion reports describe ISTF test procedures and ice-making efficiency test results that are common to many of the units tested.

1. INTRODUCTION

Commercial air conditioning loads are a large component of the afternoon peak loads served by electric utilities. Increased use of cool storage would shift this electrical load from peak to off-peak periods. This shift would permit utilities to defer construction of additional generating capacity and reduce customers' demand charges.

Although the number of cool storage installations in commercial buildings is growing, it represents only a small fraction of the potential market. One major barrier to the use of cool storage equipment has been the uncertainty associated with the performance of this

*Units used throughout this report are common to and exclusive in the industry.

equipment. Uniform testing by an independent agency has not been available. The performance data available from manufacturers are varied in scope and detail from one type of device to another and across manufacturers as well. Often system performance values are given for only one operating point, making it difficult to predict performance under other operating conditions.

Electric Power Research Institute (EPRI) therefore sponsored the development of an Ice Storage Test Facility (ISTF) to permit uniform testing of commercial-size cool storage equipment of many different types. This testing serves two purposes: (1) to provide uniform performance test results and (2) to promote system improvements based on experimental data. Uniform test results will be useful to utilities in promoting their installation and use, to utilities in requesting rate incentives from public utilities commission (PUCs), and to building designers in specifying appropriate equipment for their applications. The experimental data will also be useful to equipment designers because it will describe component behavior as well as overall system performance. Toward these ends, the ISTF was designed with the capability to test dynamic, liquid recirculation, secondary fluid, and direct expansion (DX) ice makers. The capacity of the test unit was sized at 250 ton-h. Real-time data acquisition and precise computer controls were included.

This report describes the test results for an ice storage tank furnished by BAC. The BAC storage tank was originally equipped with a coil designed for a liquid-overfeed refrigeration system. After several tests were run on this system, the liquid-overfeed coil was removed, and a brine coil was installed in the same tank. For both coils, the tank was discharged using an external melt arrangement. The storage system and the test facility are described in Sect. 2. Section 3 describes the tests that were performed to characterize the storage system, and Sect. 4 describes the analysis methods used to evaluate the performance data. The test results are discussed in Sect. 5, and recommendations are summarized in Sect. 6.

2. SYSTEM DESCRIPTION

2.1 BAC STORAGE SYSTEM

The BAC TSU-275B ice tank (~8 ft wide by 14 ft long by 8 ft tall) is chilled by the flow of either liquid refrigerant or brine through serpentine coils submerged in water. In a liquid-overfeed system, a portion of the refrigerant vaporizes, thereby absorbing heat from the water and forming ice (to a design thickness of 1.4 in.) on the exterior surface of the coils. A sufficient amount of refrigerant is forced into the coils to ensure a wetted interior tube surface throughout the length of the tube, which provides greater heat transfer and ice storage surface than can be obtained with traditional DX coils. A chilled brine solution can also be used to absorb heat from the water and form ice (again, to a design thickness of 1.4 in.) on the exterior surface of coils designed for this application. The brine used for these tests was a mixture of ethylene glycol and water with a freezing point of ~0°F. BAC recommends a mixture with a slightly higher freezing point.

The BAC ice tank is discharged by circulating the water in the tank through an external heat load, simulated by a simple heater in the test facility. It is therefore important not to freeze the tank fully solid but to leave enough free water to ensure adequate water circulation passages within the ice tank. The ice tank is equipped with an ice thickness sensor that can be used to select the amount of ice stored during a charging cycle.[1] However, the sensor is not designed to provide information during a discharge cycle and may not be accurate when recharging after a partial melt.

Air agitation is used with the BAC storage tank to ensure adequate water mixing during the discharge cycle and in the chilling portion of any charging cycle. Once the tubes are covered with a layer of ice during the charging cycle, the agitation is not required. The agitation air compressor was usually turned off when the tank was ~20% charged, per BAC's recommendation.

When the BAC tank was filled to the recommended level of 69.25 in., it held about 4500 gal of water. The BAC literature gives a water volume of 5400 gal. The value in the BAC literature is based on the maximum water depth that could occur before the tank overflows and therefore corresponds to the maximum operating weight. The coil volumes, both brine and liquid overfeed, were not measured.

2.2 TEST FACILITY

The test facility was designed to test a wide variety of storage systems. It includes all refrigeration system components necessary to charge both liquid-overfeed and brine systems. Figure 1 shows the test facility configuration used to test the BAC ice storage tank equipped with the liquid-overfeed coils. Figure 2 shows the configuration used to test the BAC storage tank equipped with the brine coils. The test facility is well-equipped with monitoring devices to measure temperature, pressure, flow, and energy use. The monitoring points shown in Figs. 1 and 2 are listed in Tables 1 and 2, respectively. A differential pressure gage (PDE1) was used to measure changes in the tank water depth that occur during freezing due to the difference in density between ice and water. Although the depth change is small relative to the overall depth of the water, it is accurately measurable by placing the differential pressure gage in a stand pipe slightly below the tank's water level. The test loop instrumentation is described more fully in Appendix A and Ref. 2.

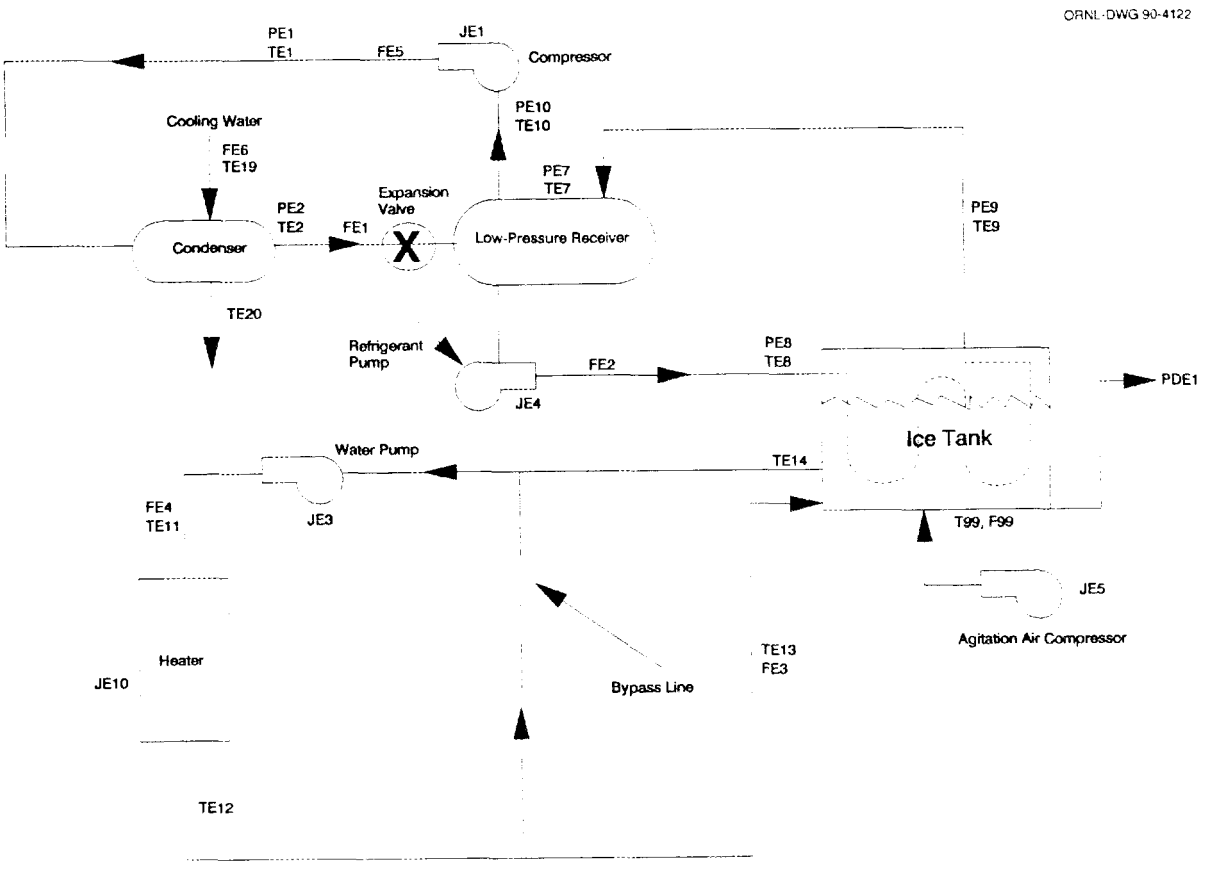

Fig. 1. ISTF schematic for BAC liquid-overfeed system.

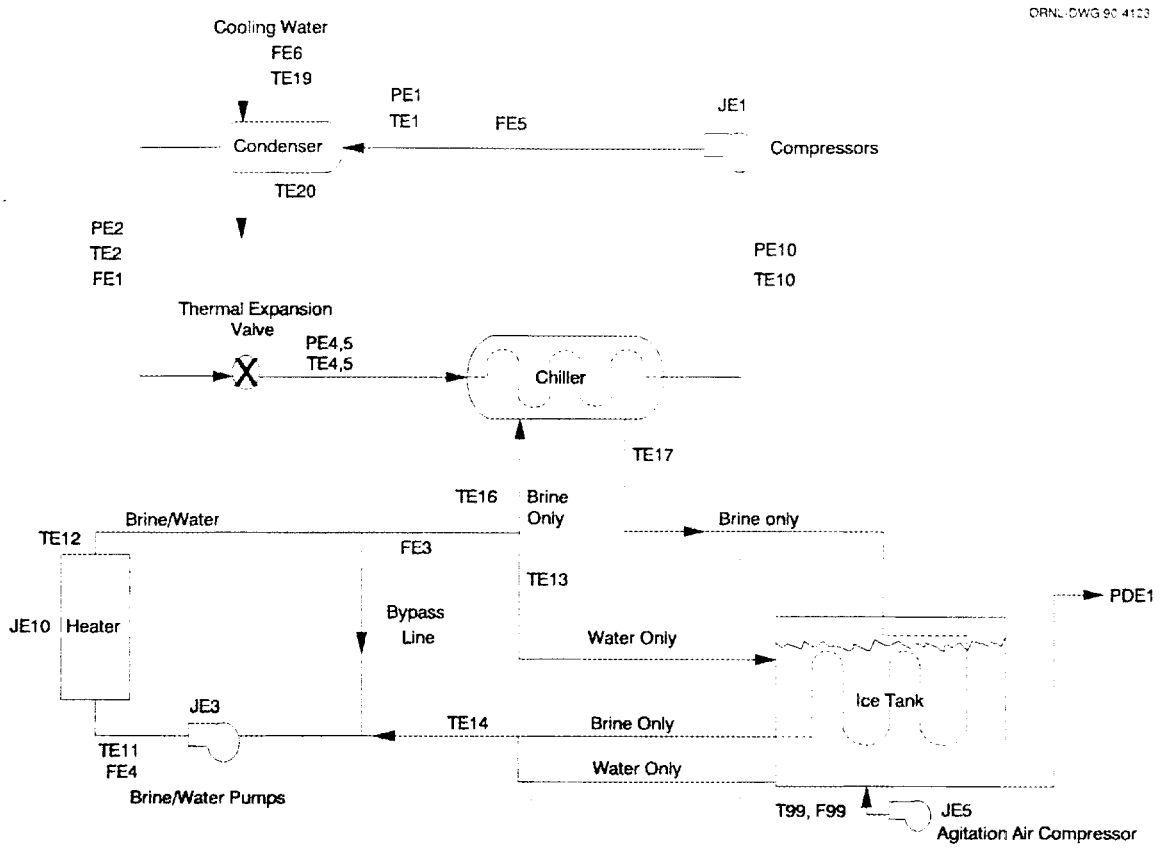

Fig. 2. ISTF schematic for BAC brine system.

The low-pressure receiver in the liquid-overfeed system (see Fig. 1) is designed for the low-velocity separation of gas and liquid refrigerant. In this function, it combines two separate refrigerant flow circuits. One circuit is comprised of the compressor, condenser, expansion valve, and receiver; the other circuit includes the refrigerant pump, ice tank coils, and receiver. A rotary positive displacement pump is used to force the liquid refrigerant into the storage tank coils. Orifice plates provided by BAC are used to balance refrigerant distribution to each refrigerant coil within the ice tank. These plates are usually sized for a particular refrigerant flow rate. However, the testing plan called for a wide range of operating conditions and refrigerant flow rates. Therefore pressure drops through these orifices were somewhat larger than would be the case had the orifices been sized for a specific refrigerant flow rate.

For the brine system, a centrifugal pump was used to circulate both brine during the charge cycle and water during the discharge cycle, as is shown in Fig. 2. The sections of piping used by both brine and water were drained, rinsed, and refilled between each charge

Table 1. ISTF monitoring points for the liquid-overfeed system

Point label	Measured quantity
FE1	Low-pressure receiver inlet flow, refrigerant
FE2	Ice tank inlet flow, refrigerant
FE3	Ice tank inlet flow, water
FE4	Heater inlet flow, water
FE5	Compressor outlet flow
FE6	Condenser inlet water flow
F99	Agitation air flow[a]
JE1	Compressor energy and power
JE3	Water pump energy and power
JE4	Refrigerant pump energy and power
JE5	Agitation air compressor power
JE10	Heater energy and power
PDE1	Differential pressure (measures tank water height)
PE1	Compressor discharge pressure
PE2	Condenser outlet receiver pressure
PE7	Low-pressure receiver pressure
PE8	Ice tank inlet refrigerant pressure
PE9	Ice tank exit refrigerant pressure
PE10	Compressor suction pressure
TE1	Compressor discharge temperature
TE2	Condenser discharge temperature
TE7	Low-pressure receiver temperature
TE8	Ice tank inlet refrigerant temperature
TE9	Ice tank outlet refrigerant temperature
TE10	Compressor suction temperature
TE11	Heater inlet water temperature
TE12	Heater outlet water temperature
TE13	Ice tank inlet water temperature
TE14	Ice tank outlet water temperature
TE19	Condenser inlet water temperature
TE20	Condenser outlet water temperature
T99	Agitation air temperature

[a]Not continuously recorded.

Table 2. ISTF monitoring points for the brine-coil system

Point label	Measured quantity
FE1	Chiller inlet flow, refrigerant
FE3	Chiller inlet flow, brine, or ice tank inlet flow, water
FE4	Brine/water pump discharge flow, water or brine
FE5	Compressor outlet flow
FE6	Condenser inlet water flow
F99	Agitation air flow[a]
JE1	Compressor energy and power
JE3	Water pump energy and power
JE5	Agitation air compressor power
JE10	Heater energy and power
PDE1	Differential pressure (measure tank water height)
PE1	Compressor discharge pressure
PE2	Condenser outlet refrigerant pressure
PE4	Chiller inlet refrigerant pressure
PE5	Chiller outlet refrigerant pressure
PE10	Compressor suction pressure
TE1	Compressor discharge temperature
TE2	Condenser discharge temperature
TE4	Chiller inlet refrigerant temperature
TE5	Chiller outlet refrigerant temperature
TE10	Compressor suction temperature
TE11	Heater inlet water temperature
TE12	Heater outlet water temperature
TE13	Ice tank inlet water temperature
TE14	Ice tank outlet water temperature
TE15	Ice tank outlet brine temperature
TE16	Ice tank inlet brine temperature
TE17	Chiller outlet brine temperature
TE18	Chiller inlet brine temperature
TE19	Condenser inlet water temperature
TE20	Condenser outlet water temperature
T99	Agitation air temperature

[a]Not continuously recorded.

and discharge cycle. The evaporator/chiller (see Fig. 2) connects the test facility's refrigeration system to the brine loop that charges the ice storage tank. In the evaporator/chiller, the refrigerant is vaporized, absorbing heat from the brine. To accommodate the desired wide range of testing conditions, a chiller with two independent

refrigerant coils was selected. The control system is designed to select one or both chiller coils based on the compressor loading. The thermal expansion valves feeding refrigerant to these coils open and close in response to the measured superheat at the coil exit. Because the evaporator/chiller was often running under part-load conditions, the thermal expansion valves exhibited a large degree of hunting during the beginning of most freeze tests. This behavior is typical of partially-loaded expansion valves; the hunting usually stopped after ~30 to 45 min of operation. The brine pump speed was varied to maintain the brine flow rate at the selected value during the charge cycle.

The ISTF was designed to permit testing under a wide range of controlled conditions. Two parallel compressors with part-load capabilities are used to vary the chiller capacity from 15 to 95 tons. The flow of water to the condenser controls the condensing temperature between 80 and 100°F. The flow of refrigerant to the ice tank in the liquid-overfeed system is controlled using a variable-speed refrigerant pump located below the low-pressure receiver. In the liquid-overfeed system, an expansion valve meters refrigerant flow from the condenser in response to the liquid level in the low-pressure receiver. During discharge cycles, the water pump speed, heater power, and bypass valve positions are used to control test conditions.

Because of the high miscibility of compressor lubricating oil in the halocarbon refrigerants, provisions must be made to provide adequate oil in the compressors.

An oil separator is located at the compressor discharge to return oil to the compressor crankcase via an oil still. In a liquid-overfeed system, oil also tends to accumulate in the low-pressure receiver because of the low temperature, low pressure, and low flow rates at this point in the cycle. Therefore, whenever the level in the oil still falls, a small amount of refrigerant/oil mixture is bled from the refrigerant pump discharge and sent to the oil still. In the still, the refrigerant is boiled off and returned to the suction line. Oil return in the brine chiller system is much simpler than with other systems tested. Although an oil still is not required, an oil reservoir between the oil separator and the compressor crankcase is recommended. Proper line sizing ensures that any oil remaining in the refrigerant is swept through the loop and returned to the compressor.

3. SYSTEM TESTS

The test plan was structured to test the storage tank's capabilities over a wide range of operating conditions. The compressor discharge pressure and loading and the brine or refrigerant flow rates were the primary variables during the charging tests. The flow rate to the heater, heater power, and the water temperature exiting the heater were the control variables during the discharge tests. Initial testing was aimed at calibrating instruments. These calibration tests were followed by a series of charge and discharge cycles aimed at characterizing the storage system performance.

During the calibration tests, the level indicator described in Sect. 2 was tested through a series of fill and drain tests with both the fill and drain water amounts measured by independent flowmeters. This established a relationship between volume and tank height. Then a series of freeze and drain tests were used in conjunction with the level indicator readings to test the BAC Ice-Logic ice thickness controller. In these tests, the system was run until the controller indicated a certain level of charge, such as 20%, had been reached. As soon as the indicator light came on, the compressor was stopped and the water in the ice tank was drained. The amount of water drained was measured, as was the water used to refill the tank. Because the original amount of water in the tank had also been measured, this measured drainage revealed the amount of ice remaining in the tank. The freeze and drain procedures were repeated multiple times at several different levels. A few of the tests produced anomalous results indicating that water was probably trapped in the ice and unable to drain. Overall, however, the tests were repeatable. The measured density of ice in these tests was 57.2 lb/ft^3, in good agreement with the reported range of 57.2 lb/ft^3 at 0°C to 57.4 lb/ft^3 at -10°C (Ref. 3). After the liquid-overfeed coils were replaced with the brine coils, data were taken during one fill and drain cycle to check this previous calibration. No changes were needed.

The test schedule was designed to show how the storage system would respond to different ice-charging periods (from 8 to 16 h). The ice-discharge tests were designed to mimic different discharge periods ranging from 6 to 12 h with varying temperature and flow requirements at the heater. Tables 3–5 are taken from the ISTF test procedure and show the desired testing schedule. However, this procedure was being revised during the BAC tests. (Indeed, many revisions were prompted by the experience gained during the BAC

Table 3. Planned charge test sequence

Test No.	Test duration (h)	Refrigerant flow to storage tank[a] (gal/min)	Brine flow to storage tank[b] (gal/min)
1	6	MR[c]	MR
2	6	1.25 × MR	1.5 × MR
3	10	MR	MR
4	14	MR	MR
5	14	0.8 × MR	0.5 × MR
6	18	MR	MR
7	10	MR	2 × MR
8	6	MR	MR

[a]Specified for liquid-overfeed tests only.

[b]Specified for secondary loop tests only.

[c]Manufacturer's recommended flow rates.

Table 4. Planned discharge test sequence

Test No.	Test duration (h)	TE12 (°F)	TE11 (°F)
1	6	60	38
2	9	60	45
3	12	60	45
4	6	50	38
5	9	50	38
6	12	50	45

Table 5. Planned standby test sequence

Test No.	Test duration (h)	Initial tank condition
1	>60	Fully frozen
2	>60	Fully frozen

tests.) Tables 6 and 7 present a summary of the tests that were used to analyze the BAC storage system performance. Many additional tests were made but are excluded from this report because of operational difficulties at the ISTF. All charge and discharge tests were planned to extend from a fully melted tank to a fully charged tank. As will be discussed later, not all tests met this goal.

The operational difficulties that limited the test execution were primarily related to the wide range of capacities that were to be tested. Compressor cooling requirements and expansion valve capacity limited the chiller capacity under certain conditions. For example, at very high compressor capacities, the suction temperature would drop low enough to trip the compressor low-pressure limit switch. The maximum heater power available limited the shortest discharge time to about 7 h. Other operational difficulties were related to debugging the ISTF control system. Despite these limitations, the completed tests are broad enough in scope to permit reliable performance estimates over a wide range of operating conditions.

Many charging tests were run under compressor part-load conditions. Comparing actual power use to the compressor curve predictions for full-load power use underscores the high efficiency penalties associated with part-load operation. These penalties are discussed further in a companion document.[4]

Shell heat gains were measured by recording the change in ice inventory over a long period of time in the absence of all external fluid flows and with the tank covers in place. The ice depletion over these time periods was ascribed to shell heat gains. Similar tests were conducted by measuring the temperature rise in a tank full of chilled water without any ice. For these tests, the water temperature was measured after a mixing period of at least 10 min, before and after a long period of time without any external fluid flows. The ambient temperature was also noted during all standby tests. However, the ambient conditions showed little variation because of the sheltered location of the test floor.

The agitation heat gains were estimated by installing a flowmeter after the agitation air compressor. The air temperature was measured before and after the air compressor. The ambient relative humidity was also measured.

Table 6. BAC charging test sequence

Test ID	Test duration (h)	Refrigerant flow to storage tank (lb/min)		Brine flow to storage tank (gal/min)
		MR[a]	Test average	
0801	12[b]	100	160	
0811	7[c]	260	240	
0815	13	140	240	
0824	15[c]	100	200	
0914	7	270	240	
0922	6	280	240	
0523	7[d]			74
0613	12			75
0619	18			75
0623	18			75
0628	12			75
0727	8			132
0731	14[e]			133
0803	10			133

[a]MR = flow rate based on manufacturer's recommended overfeed ratio of 3/1 and average measured saturated suction temperature.

[b]Test ended when the tank was ~70% charged.

[c]Test began when the tank was ~20% charged.

[d]Test began when the tank was ~40% charged.

[e]Test was stopped when the tank was 94% charged.

Table 7. BAC discharge test sequence

Test ID	Test duration[a] (h)	Temperature (°F)		
		Discharge rate[b] (tons)	To load	From load
0825	11	24	*c*	*c*
0913	11	*d*	38	45[e]
0915	8	33	38	45[e]
0524	8	36	42	50
0608	11		41	50
0620	9	33	43	50
0626	7	35	37	50
0629	9	33	54	60
0707	8	37	47	60
0712	12	28	52	60

[a]End of test defined in this table as time when storage tank outlet temperature exceeded 44°F.

[b]Based on water flow and tempeatures at the tank, corrected.

[c]Uncontrolled; flow rate was a constant 33 gal/min.

[d]Uncorrected due to instrument malfunction.

[e]Allowed to rise when water exiting ice tank exceeded 38°F.

4. ANALYSIS METHODOLOGY

The primary concern of the data analysis is to produce useful information and to present it in a meaningful fashion. Another concern is to distinguish between the performance of the ice storage system and the performance of the refrigeration system. While analysis of the refrigeration system performance can prove enlightening and is certainly useful to system designers, it must be distinguished from that of the manufacturer's storage system. Also, the test facility is different from a commercial system because it must have the flexibility to test a wide variety of system types. This introduces much added complexity that a commercial system would not encounter.

4.1 DATA PROCESSING

The data available for each operational test permit redundant calculations that increase our understanding and confidence in the test results. For example, the heat rejection at the condenser is measured on both the water and refrigerant sides of the heat exchanger. The refrigeration effect to the ice tank is measured by both changes in the water height (a measure of the ice inventory) and by either the refrigerant flow and enthalpy change across the low-pressure receiver, for the liquid-overfeed system, or the brine flow and temperature change, for a brine system. Also for a brine system, the refrigeration effect is measured at the chiller on both the brine and refrigerant sides. The energy available for discharge is measured by water flow and temperatures at the heater and at the ice tank, as well as by monitoring the change in the storage tank water height and the power going to the discharge heater. This duplication of measurements also enables us to more fully separate the performance of the ice storage system from that of the refrigeration system.

The data are collected for each monitoring point every 30 s during a charge test and every 15 s during a discharge test. This collection frequency is dictated by system control requirements rather than by the analysis requirements. The data are immediately summed (for flows or energy uses) or averaged (for temperatures, pressures, power uses, and flow rates) to represent the appropriate values on a 5-min basis.

Thermodynamic properties for R-22 are calculated from a computerized format developed by G. T. Kartsounes and R. A. Erth and adapted for use at Oak Ridge National

Laboratory (ORNL) by C. K. Rice and S. K. Fischer.[5] Brine properties, as a function of concentration and temperature, were provided by the Union Carbide Company, and information for the temperature range of interest was extracted.[6]

4.2 REFRIGERATION EFFECT

The refrigeration effect in the ice tank is directly measured by recording the depth of the water in the tank, as was described in Sect. 3. This measurement is reliable whenever ice is present in the tank and the ice is submerged, which are usual conditions during a charging cycle. Because of the accuracy of the differential pressure monitor used for this measurement, the change in water depth is best used over relatively long periods of time, such as 30 min or more. It is therefore better suited for providing a cumulative measure of the latent energy stored in the ice tank than for providing an instantaneous measure of system capacity.

4.2.1 Liquid-Overfeed Coils

Refrigerant measurements at the ice tank are hampered by the inability to measure the quality of the exit flow and by not knowing the exact proportion of oil in the liquid refrigerant flow (although available miscibility diagrams indicate that ~5% of the liquid circulated is oil).[7] However, refrigerant measurements at the low-pressure receiver can be used to measure the refrigeration effect if given a few simplifying assumptions. These assumptions include (1) a constant liquid level in the receiver (true for long periods of time, less true for short periods of time); (2) low gas and liquid velocities in the receiver; (3) no shell losses (the receiver was well insulated); (4) no thermal losses at the metering expansion valve (i.e., adiabatic expansion); (5) steady flow; (6) no significant pressure drops in the liquid piping; and (7) no energy gains in the liquid piping outside the ice tank. Under these assumptions, the refrigeration effect is shown in Eq. (1). Shell heat gains to the tank, air agitation heat gains, and refrigerant pump energy are subtracted because this portion of the refrigeration effect is unavailable to make ice. These heat gains are discussed more fully later in this section.

$$RE_f = FE1 \times (1 - X_3) \times h_{fg} - (\text{shell} + \text{agit} + JE4) , \qquad (1)$$

where

RE_f = refrigeration effect as determined by the refrigerant flow rates and thermodynamic properties,

FE1 = refrigerant flow from the condenser,

X_3 = quality of refrigerant after the expansion valve (established by the refrigerant pressure and temperature at the condenser outlet and by the evaporating temperature),

h_{fg} = enthalpy of evaporation at the refrigerant pressure in the low-pressure receiver,

shell = heat gains through the ice storage tank shell,

agit = heat gains due to the agitation air flow into the ice tank,

JE4 = heat added by the refrigerant pump.

Based on comparison to the change in tank water depth, this calculation and its imbedded assumptions tended to overpredict the refrigeration effect, as will be discussed further in Sect. 5. The impact of the first assumption was investigated by comparing the results for data aggregated over 5-min, 10-min, and 1-h time periods. The cumulative refrigeration predicted for each of these aggregation levels was essentially identical, lending confidence in this assumption. It is more difficult to measure the errors introduced by the other assumptions. Noticeable during operation were refrigerant flow fluctuations that could indicate errors introduced by the steady flow assumption. Coil pressure drops were reasonable and varied from 6 to 9 psi, due to the orifice plate sizing as is further discussed in Sect. 5.1.1.

These two primary methods (water level and refrigerant measurements) of measuring the refrigeration effect to the tank had different advantages. The refrigerant measurements accurately reflected changes in the charging rate for very short periods of time. The change in water depth provided the most accurate measure of total tank charge over a longer time frame. These two measures were combined into a "corrected" instantaneous capacity as is shown in Eq. (2).

$$RE^*_f = RE_f \times (\overline{RE_w}/\overline{RE_f}) , \qquad (2)$$

where

Re_f^* = corrected capacity,

$\overline{Re}_w$ = capacity based on water depth change averaged over the test period,

$\overline{Re}_f$ = capacity based on refrigerant measurement averaged over the test period.

This corrected capacity can be used to calculate the quality of the refrigerant gas exiting the ice tank [Eq.(3)], and therefore to define the actual liquid-overfeed ratio used [Eq. (4)].

$$X_9 = [Re^*_f + \text{shell} + \text{agitation} + JE4] / [h_{fg} (1 - P) \times FE2] , \tag{3}$$

$$LOR = 1/X_9 , \tag{4}$$

where

X_9 = refrigerant quality at the ice tank exit,

P = oil fraction refrigerant flow to the ice tank, assumed value of 0.05,

LOR = liquid overfeed ratio,

JE4 = heat added by the refrigerant pump, and

FE2 = refrigerant flow to the ice tank.

The shell and agitation heat gains must be added to the corrected capacity because this calculation is focused on the cooling performed by the refrigerant rather than the refrigeration available to make ice. An assumed oil content of 5% of the liquid flow was used for this calculation. No change was assumed in the oil enthalpy as it traveled through the ice tank.

4.2.2 Brine Coils

The refrigeration effect is calculated from the measured brine flow rate and temperature gain as is shown in Eq. (5). Shell heat gains to the tank and air agitation heat gains are subtracted because this portion of the refrigeration is unavailable to make ice.

$$RE_b = FE4 \times c_p \times \rho \, (TE15 - TE16) - (\text{shell} + \text{agitation}) , \tag{5}$$

where

RE_b = refrigeration effect measured by the brine,
FE4 = brine flow from the chiller,
c_p = brine specific heat,
ρ = brine density
TE15 = brine temperature leaving the ice tank,
TE16 = brine temperature entering the ice tank,
shell = heat gains through the tank shell,
agitation = heat gains due to the agitation air flow.

The brine specific heat and specific gravity are provided in the form of families of curves in Ref. 4. Interpolations from these curves for the temperature range from 20 to 60°F and a brine concentration of 33 wt % produced the following equations for specific gravity (relative to water at 60°F) and specific heat.

$$SG = (-0.0002) \times T + 1.063 , \tag{6}$$

where

SG = specific gravity,
T = average brine temperature, °F.

$$c_p = 0.0003 \times T + 0.899 , \tag{7}$$

where c_p is specific heat, Btu/(lb-°F). Based on comparison to the change in tank water depth, this calculation and its imbedded assumptions tended to overpredict the refrigeration effect at the lower brine flow rate and to underpredict the effect for tests at the higher flow rate. To account for these errors, a correction factor was determined by comparing the average measured capacity from the brine (during the ice-producing portion of the tests) and the change in tank water depth. The "corrected" instantaneous capacity Re^*_b was defined as

$$Re^*_b = Re_b \times (\overline{Re}_w/\overline{Re}_b) , \tag{8}$$

where

Re_b^* = corrected capacity,

$\overline{Re}_w$ = capacity based on water depth change, averaged over the test period,

$\overline{Re}_b$ = capacity based on brine measurement, averaged over the test period.

The system capacity was also measured at the evaporator/chiller on both the brine and refrigerant sides. These measurements provided another checkpoint to guard against loss of data if one instrument fails. The capacity measured at the chiller is expected to be slightly higher than that at the ice tank because of shell heat gains at the tank and in the piping and also by energy added by the brine pumps and air agitation. The brine-side measurements are similar to those used for the ice tank and are shown in Eq. (9).

$$RE_{bch} = FE4 \times c_p \times \rho \times (TE18 - TE17) , \tag{9}$$

where

RE_{bch} = refrigeration effect at the chiller, based on brine flow and temperature measurements,

FE4 = brine flow from the chiller,

c_p = brine specific heat,

ρ = brine density,

TE17 = brine temperature leaving the chiller, and

TE18 = brine temperature entering the chiller.

The refrigerant-side measurements are used in Eq. (10). Shell losses from the well-insulated chiller are assumed to be negligible.

$$RE_{fch} = FE1 \times (HE10 - HE2) , \tag{10}$$

where

FE1 = refrigerant flow to the chiller,

HE10 = enthalpy corresponding to the measured suction temperature and pressure of the superheated refrigerant leaving the chiller,

HE2 = enthalpy corresponding to the saturated liquid refrigerant leaving the condenser.

4.2.3 Refrigeration System

Another measurement of the system capacity can be taken from the compressor curves provided by the manufacturer. These curves were modeled as,

$$Re_c = 49.35 + 1.663 \times T_s - 0.00173 \times (T_d)^2 - 0.00708 \times T_s \times T_d + 0.00953 \times (T_s)^2 , \quad (11)$$

$$\dot{W} = 44.088 - 0.508 \times T_s + 0.000840 \times (T_d)^2 + 0.0123 \times T_s \times T_d - 0.00592 \times (T_s)^2 , \quad (12)$$

$$\dot{Q} = 1.090 - 0.00422 \times T_s + 0.00263 \times T_d , \quad (13)$$

where

Re_c = refrigeration capacity predicted by the compressor capacity curves, tons;
T_s = saturated suction temperature, °F;
T_d = saturated discharge temperature, °F;
$\dot{W}$ = compressor power predicted by the manufacturer's data, Bhp;
$\dot{Q}$ = heat of rejection predicted by the compressor manufacturer, tons.

Equation (11) predictions match the compressor manufacturer's table within ± 0.5 tons. Equation (12) predictions match the manufacturer's table within ± 0.5 Bhp. The heat of rejection model, Eq. (13), has residuals ranging from -0.005 to $+0.016$. All of the liquid-overfeed tests were run at part-load conditions; that is, the compressor was not operating at full capacity. The compressor curve capacity and heat rejection predictions were therefore ratioed according to the loading on the compressor. The manufacturer's power consumption table is good only for fully loaded conditions and cannot meaningfully predict part-load power requirements.

As another check on the system, the heat rejected at the condenser is measured on both the refrigerant and water sides as

$$\dot{Q}_w = FE6 \times (TE20 - TE19) , \quad (14)$$

$$\dot{Q}_f = FE5/VE1 \times (HE1 - HE2)\,, \tag{15}$$

where

$\dot{Q}_w$ = heat absorbed by the cooling water,
FE6 = water flow rate,
TE20 = water temperature into the condenser,
TE19 = water temperature exiting the condenser,
$\dot{Q}_f$ = heat rejected by the refrigerant,
FE5 = refrigerant volume flow entering the condenser,
VE1 = refrigerant specific volume entering the condenser,
HE1 = refrigerant enthalpy entering the condenser,
HE2 = refrigerant enthalpy leaving the condenser.

4.2.4 Capacity Models and Capacity Normalization

A normalized capacity is also calculated to provide a clearer picture of the change in capacity during the charging cycle. The capacity at each point in time is divided by the average capacity over the entire charging test period (not including the cooldown portion of the test). The normalization is only accurate for those tests that extend from the fully melted to the fully frozen states. Because several tests began from a partially frozen state or ended before the tank was fully charged, another step was necessary before the capacity could be normalized for these partial tests.

This intermediate step consisted of creating a mathematical model of the capacity as a function of the state of charge for each point in time during the test. Several models were tested using the SAS Institute's system procedure entitled REG.[6] This procedure fits least-squares estimates to linear regression models and reports the adjusted squared correlation coefficient as well as the Student's t-ratio and significance probability for each parameter estimate. Based on these model evaluation points, the best model was chosen and is shown in Eq. (16). The predicted values were plotted vs the residual values to check for unwanted trends in the model output.

$$Re_f = A_1 + A_2 \times PDE1 + A_3 \times (DPDE1)^2 + A_4 \times \sqrt{DPDE1}\,, \tag{16}$$

where

$A_1 - A4$ = parameter coefficients different for each test,

PDE1 = tank water depth,

DPDE1 = difference between the tank water depth and the fully melted tank water depth.

The model results were used in two ways. First, they were used to artificially extend the data set so that each test contained capacity vs state of charge data from the fully melted to the fully frozen state. In this application, the model is not used wherever actual data are available, but only to fill in data where a test began later than at a fully melted state or ended before a fully frozen state. This extended profile was then used to calculate the average capacity during the test, which was in turn used to normalize the instantaneous capacity throughout the extended test data. Second, the model was used to artificially replace the data set's capacity vs state of charge values, which were then normalized relative to the mean of the artificial data. The difference between these two uses is shown clearly in Sect. 5.

4.3 DISCHARGE ENERGY AVAILABLE

The cool storage available to meet a cooling load was measured by the water flow rates and temperature changes at the heater and at the ice tank [see Eqs.(17) and (18)]. The cool storage in the tank is also depleted by the tank's shell heat gains and by the agitation air. The cooling delivered from the ice tank is therefore equal to the change in tank storage inventory minus the shell heat and agitation gains. This will differ from the cooling delivered to the load by the amount of the pump work on the fluid.

$$cap_h = FE4 \times (TE12 - TE11) \times c_p \times \rho \,, \tag{17}$$

$$cap_t = FE3 \times (TE13 - TE14) \times c_p \times \rho \,, \tag{18}$$

where

cap_h = discharge capacity measured at the heater,

FE4 = water flow to heater,

TE12 = water temperature leaving heater,

TE11 = water temperature entering heater,

c_p = specific heat of water,

ρ = density of water,

cap_t = discharge capacity measured at the ice tank,

FE3 = water flow to ice tank,

TE13 = water temperature to ice tank,

TE14 = water temperature leaving ice tank.

The tank storage inventory is calculated based on the water depth, which gives the ice inventory, and the outlet water temperature, which is assumed to equal the mixed tank water temperature. The heater power was also measured but is not considered accurate as is discussed in Appendix A. The cumulative change in the storage tank inventory was used to correct the rates based on measured temperatures. This correction is shown in Eqs. (19) and (20) and was necessary due to temperature measurement accuracy limitations, especially for those tests with high water flow rates and correspondingly smaller temperature changes. Corrections were also made to the calculated cumulative discharge to account for standby losses that occurred whenever a test was stopped and then restarted the next day. The tank was considered to be fully discharged when the tank outlet temperature reached 44°F. Some ice may remain in the tank at that time but is unavailable to meet the load. BAC defines the end of a melt to occur sooner, when the remaining latent storage present in the ice is just sufficient to return the mixed tank water temperature to 32°F. The discharge capacity presented here will therefore be greater than BAC's rating because it will include a credit for some sensible storage.

$$\Sigma \text{ avail} = \Sigma \text{ lat} + \Sigma \text{ sens} - \Sigma \text{ shell} - \Sigma \text{ agit} - \Sigma \text{ stby}, \tag{19}$$

where

Σ avail = cumulative energy discharged from the tank and available to the load,

Σ lat = cumulative latent energy discharged from the tank,

Σ sens = cumulative sensible energy discharged from the tank,

Σ shell = cumulative energy absorbed through the tank shell at a rate of 0.5 ton,

Σ agit = cumulative energy added to the tank by the agitation air at a rate of 0.23 ton,

Σ stby = shell and piping heat gains that occur during a standby period.

$$cap^*_t = cap_t \times (\Sigma\ avail/\Sigma\ cap_t)\ , \tag{20}$$

where

cap_t^* = corrected discharge capacity measured at the tank,

$\Sigma\ cap_t$ = cumulative discharge capacity measured at the tank.

4.4 SHELL AND AGITATION HEAT GAINS

Shell heat gains were measured directly from changes in tank water depth over extended periods of time when there was no external flow.

Agitation heat gains were calculated using the measured air flow rate and temperature at the air pump following the method outlined in the *ASHRAE Fundamentals Handbook.*[7] The air leaving the top of the ice tank was assumed to be saturated at 32°F. The measured relative humidity showed some daily variation, but a representative value of 56% at an ambient temperature of 80°F (from June 21, 1988) was used for this calculation. During early monitoring, the air flow rate (19.25 ft^3/min) and inlet air temperature (125°F) were found to be essentially constant. Therefore, the air pump power was monitored and the agitation heat gain was treated as a constant value of 0.23 ton whenever the air compressor was on.

5. RESULTS

5.1 CHARGING PERFORMANCE

When designing a thermal storage system for a given application, the heat rejection temperature, storage capacity, and time available for charging are usually known.[8] This establishes the average capacity needed during the charging cycle. The ability of a storage system to meet these requirements is a function of both the storage tank/coil design and of the balance of the refrigeration system, most importantly the compressor.

Compressor manufacturers present their capacity as a function of saturated suction and discharge temperatures (Sect. 4.2 described the manufacturer's compressor data for the ISTF compressor). When charging an ice-on-coil storage tank, the suction temperature gradually drops as the water in the tank becomes colder and ice builds up on the coils. This is true for both the liquid-overfeed and the brine systems. The reduced suction temperature leads to a reduced refrigeration capacity. The rate at which the temperature drops will be determined by both the rate of charging and the amount of ice present on the coils. By showing the temperature profile of the fluid (either brine or refrigerant) entering the tank vs the tank state of charge, the effect of charging rate can be seen more clearly.

5.1.1 Liquid-Overfeed Coils

Capacity calculations were described in Sect. 4.2.1 and are based on an energy balance on the low-pressure receiver. However, in comparing the calculated refrigeration capacity to the change in storage tank depth, discrepancies are apparent. These differences range from 7 to 80% over the many tests. Also, the heat rejection measured on the refrigerant side of the condenser averaged 34% higher than that measured on the water side. A close examination of the energy balances on these cycle components led to the conclusion that the most likely source of the errors is the refrigerant flowmeters. (This examination is discussed more fully in Appendix A.) Therefore, all capacity results presented here have been corrected to agree with the measured change in ice inventory in the storage tank as was described in Sect. 4. The corrected capacity of each liquid-overfeed charge test is shown in Fig. 3. Test 0824 began with a significant amount of ice already present in the tank. Other tests, including 0922, 0914, and 0811 actually began with fully melted tanks. However, during

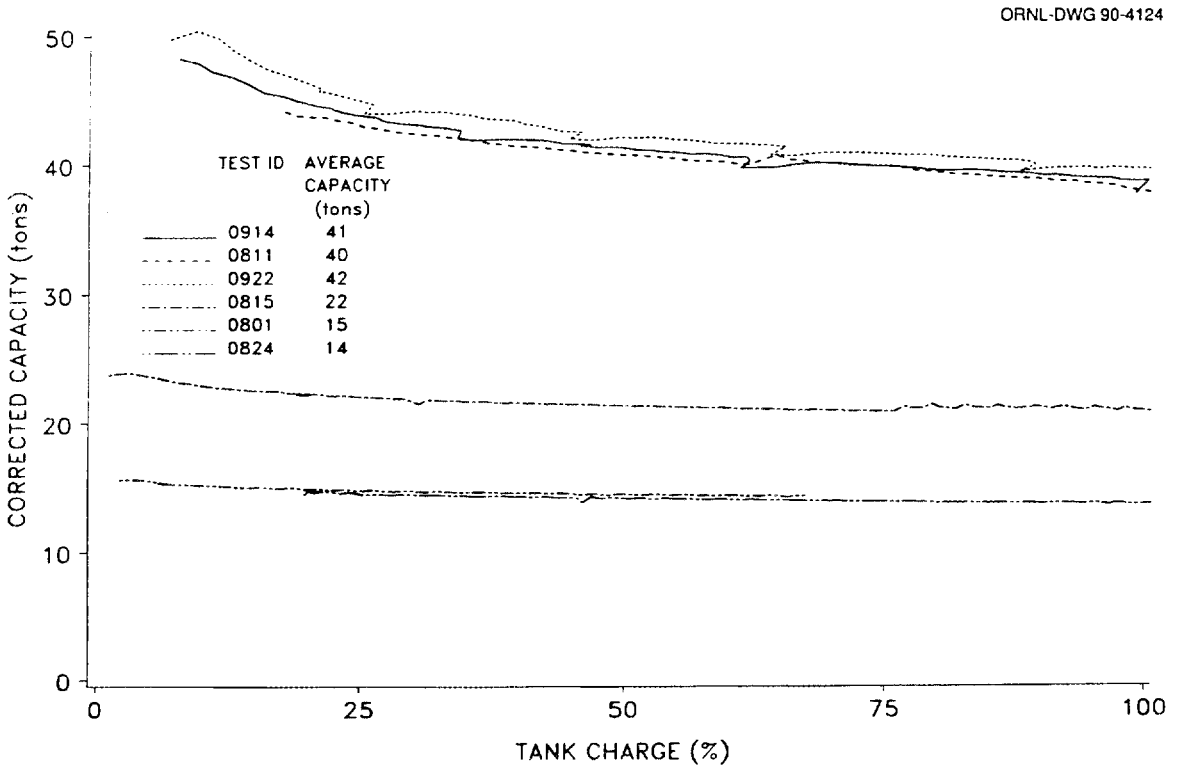

Fig. 3. Summary of corrected capacity profiles for BAC liquid-overfeed system tests.

the startup of these tests, there were control problems unrelated to the ice storage system. The data for these poorly controlled periods were deleted from this presentation to avoid confusion.

A slight decrease in capacity during the charge cycle is most apparent in those tests run at the higher rates of more than 40 tons. The tests run at 15 to 25 tons show very little change in capacity. A normalized (relative to average) capacity was calculated to show more clearly the variation in capacity during the charge cycle and is shown in Fig. 4. Because the mathematical models (discussed more fully in Sect. 4) used to extend test data from the 0 to 100% charge states are an integral part of the normalization, they deserve close examination. The adjusted squared correlation coefficient, measures of parameter significance, and plots of residuals vs predicted values were examined to verify the mathematical models. These mathematical models all had adjusted squared correlation coefficients >0.97; indeed, four of the six had adjusted squared correlation coefficients >0.99. The T-test results for the parameter estimates were >0.999 for all estimates except the PDE1SQ estimate for test 0815, which was 0.92. A more intuitive check on the models can be made by examining the results

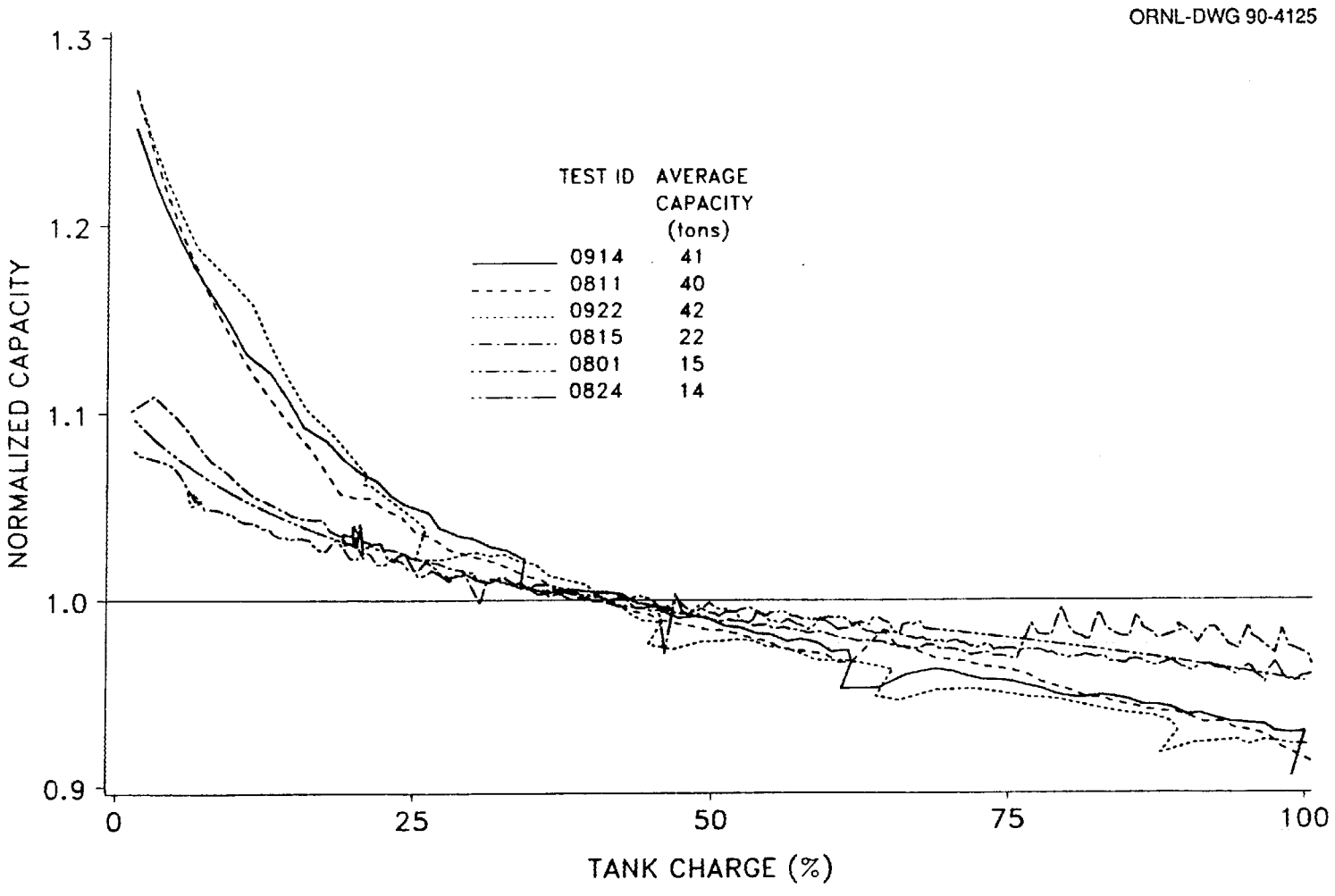

Fig. 4. Capacity of liquid-overfeed charge tests extended using test-specific mathematical models of the capacity as a function of tank charge, normalized relative to average for each test.

for tests labeled 0801 and 0824. Both of these tests were run under very similar conditions at a capacity of ~15 tons. As Fig. 3 shows, test 0801 stopped when the tank was only ~70% charged, and test 0824 started when the tank was already ~20% charged. The mathematical models were therefore used to "fill in" the end of test 0801 and the beginning of test 0824 for the profiles shown in Fig. 4. These predicted values show a smoother curve but are very close in magnitude and curvature to the actual data from the similar test. A comparison of tests 0914 and 0811 in Figs. 3 and 4 also shows that the mathematical model provides a reasonable estimate of the capacity beyond the actual test data. Once a satisfactory model is developed, it can also be used to generate a separate, artificial data set, thereby smoothing out the irregularities of the normalized capacity profiles, as is shown in Fig. 5.

Given the good model correlations, it is reasonable to use Fig. 5 to evaluate the limits of the normalized capacity as well as the crossover point at which the capacity drops below the average value. As expected, the lower capacity tests show much less variation in capacity, starting at a capacity ~10% greater than the average and ending at a capacity only ~3% less

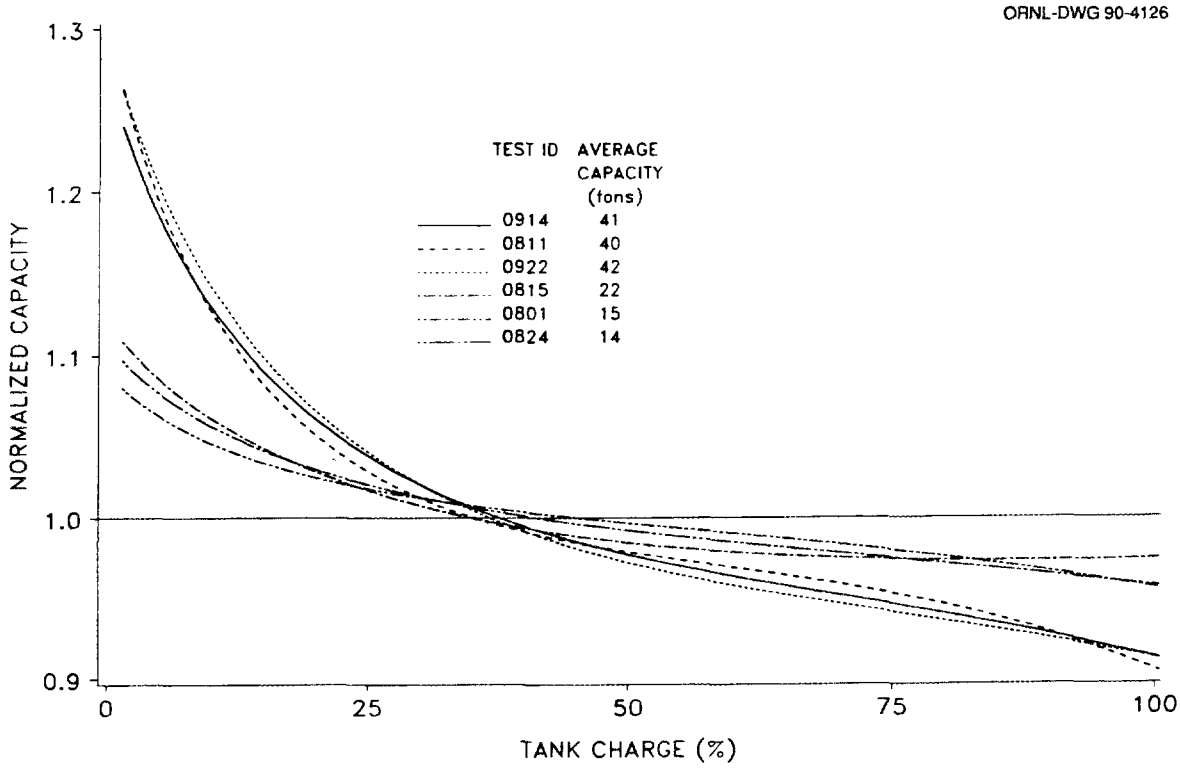

Fig. 5. Capacity of liquid-overfeed charge tests, generated by test-specific mathematical models of capacity as function of tank charge, normalized relative to average for each test.

than the average. These slower charging rates also charge up to almost 45% of the tank before dropping below the average capacity. The faster charging rates show a much greater variation in capacity, quickly dropping from a capacity 25% greater than the average down to ~5% greater than the average, while storing the first quarter of the charge and then gradually leveling off to the point where the final rate is ~8% less than the average.

The decrease in capacity during a charge cycle is caused by the reduction in saturated suction temperature caused by the increased thermal resistance of the ice layer building on the heat exchanger tubes. The saturated suction temperatures are shown vs the tank state of charge in Fig. 6 and, as expected, are much colder for the faster charge tests. The saturated suction temperatures shown in this figure are based on the refrigerant pressure at the tank outlet. The saturated suction temperature near the compressor varied from 0.1 to 1.0°F colder than that measured at the tank.

The cumulative capacity for each charge test is shown in Fig. 7. This figure shows there was no difficulty in fully charging the storage system over a wide range of charging rates, where the difference in rates is seen as the difference in the slopes of the cumulative capacity lines. The one test that stopped short of a full charge, 0801, was stopped prematurely by the operator but could have continued to a full charge without difficulty, as is shown by test 0824, which was run at the same charging rate.

To aid customers in selecting the proper compressor, BAC provides the average evaporator temperature during charge cycles of varying durations. Figure 8 shows a comparison of the values given by BAC and those measured during the tests. BAC cautions against any extrapolation beyond the given range of 10 to 14 h build time.[1] The test data presented are the average saturated temperatures at the tank exit pressure and are in close agreement with the BAC data. Due to the complexity of any given ice storage application, BAC also runs an in-house computer model for each customer. A comparison of the model predictions to test results is discussed in Appendix B.

Traditional compressor curves provide adequate guidance when selecting compressors for constant temperature systems, such as air conditioners, but are less useful for ice storage systems where the saturated suction temperature changes as charging proceeds. The test data were therefore analyzed with the aim of aiding system designers in predicting system performance with variable suction temperatures. The test data were correlated with the tank state-of-charge (relative to the rated full charge). The state of charge was chosen so that the results could be used for tanks of similar design but with different storage capacities.

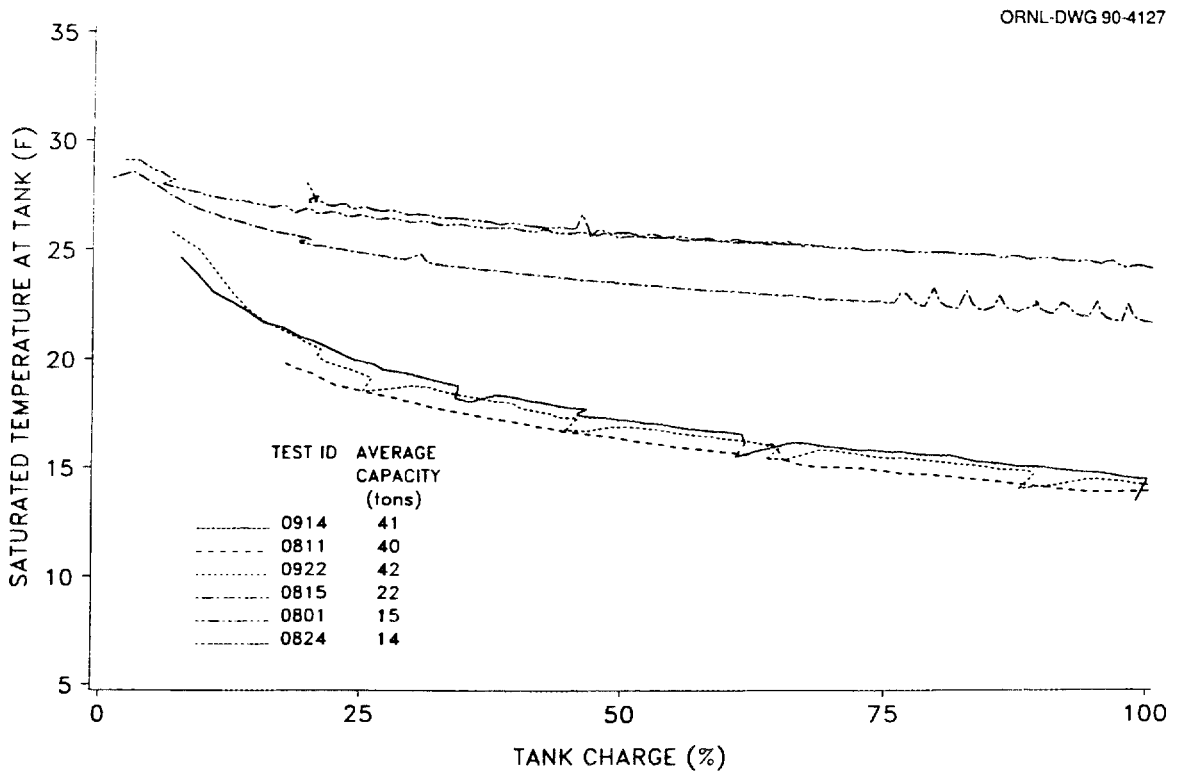

Fig. 6. Suction temperature profile summary for all liquid-overfeed charging tests. All temperature measurements are ±0.5°F.

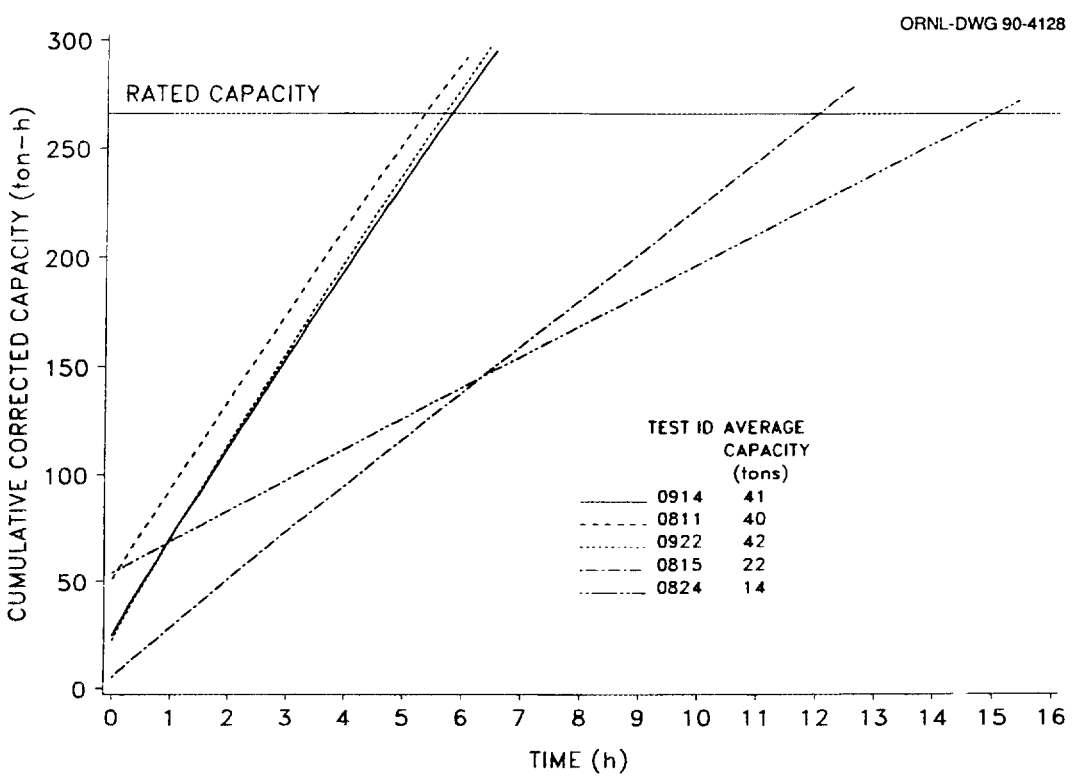

Fig. 7. Cumulative corrected capacity profile summary for all liquid-overfeed charging tests.

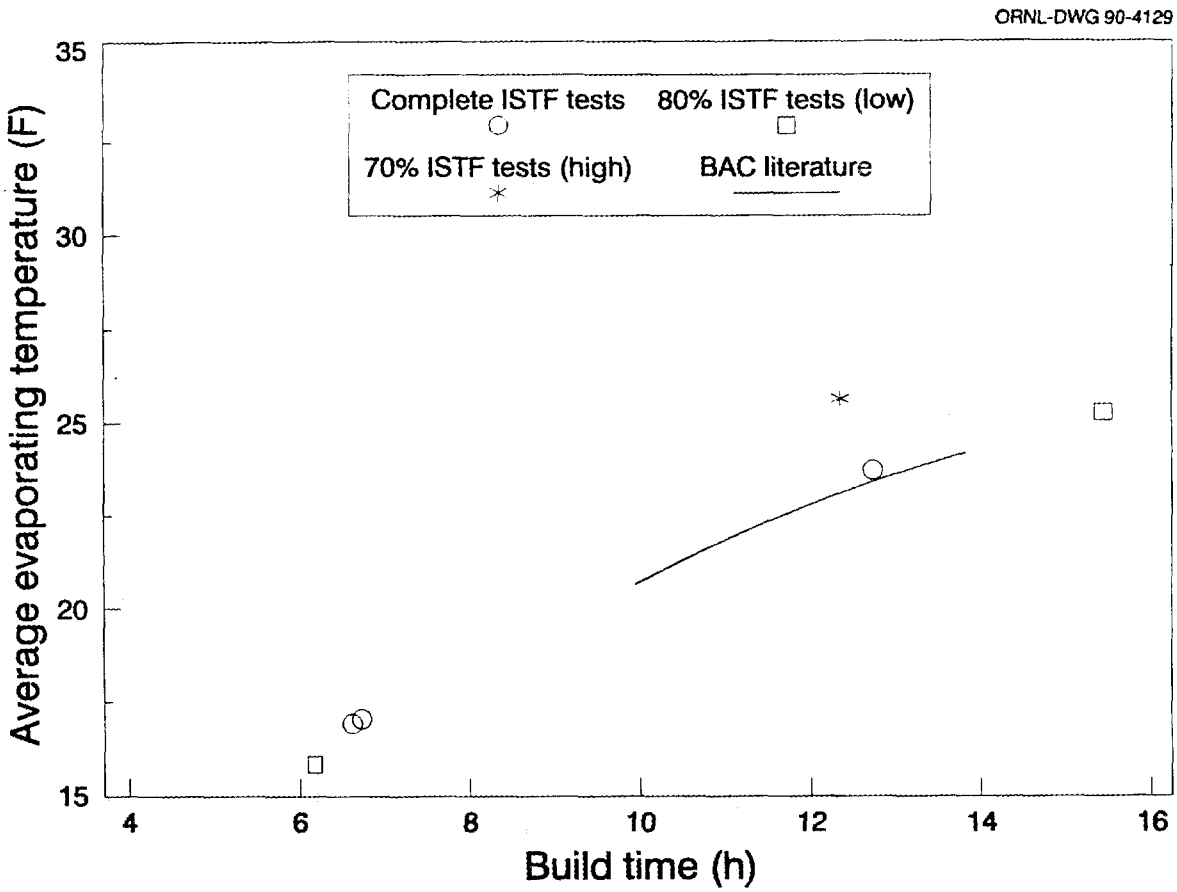

Fig. 8. Average evaporator temperature vs ice build time for BAC liquid-overfeed coils. All temperature measurements are ±0.5°F.

While Fig. 8 showed the evaporator temperature averaged over the entire charging period, Fig. 9 shows the system capacity vs suction temperature for the ice tank at 10, 25, 50, 75, and 100% charged. The state of charge is based on the measured change in tank water depth. If a manufacturer's compressor curve for a given discharge pressure is placed on top of this graph, the charging capacity and suction conditions can be approximated by the intersections of the manufacturer's curve and the linear regressions developed from the test data. (Several forms of quadratic and cubic regressions were applied to the data, but none offered any better fit than the linear model shown.) The average capacity for that given compressor under ice-making conditions can then be estimated.

The advantage to the liquid-overfeed system is the enhanced heat transfer available with a fully wetted tube and the fact that the entire tube surface is used to build and store ice. The manufacturer recommends a liquid-overfeed ratio of 3 for this particular system.

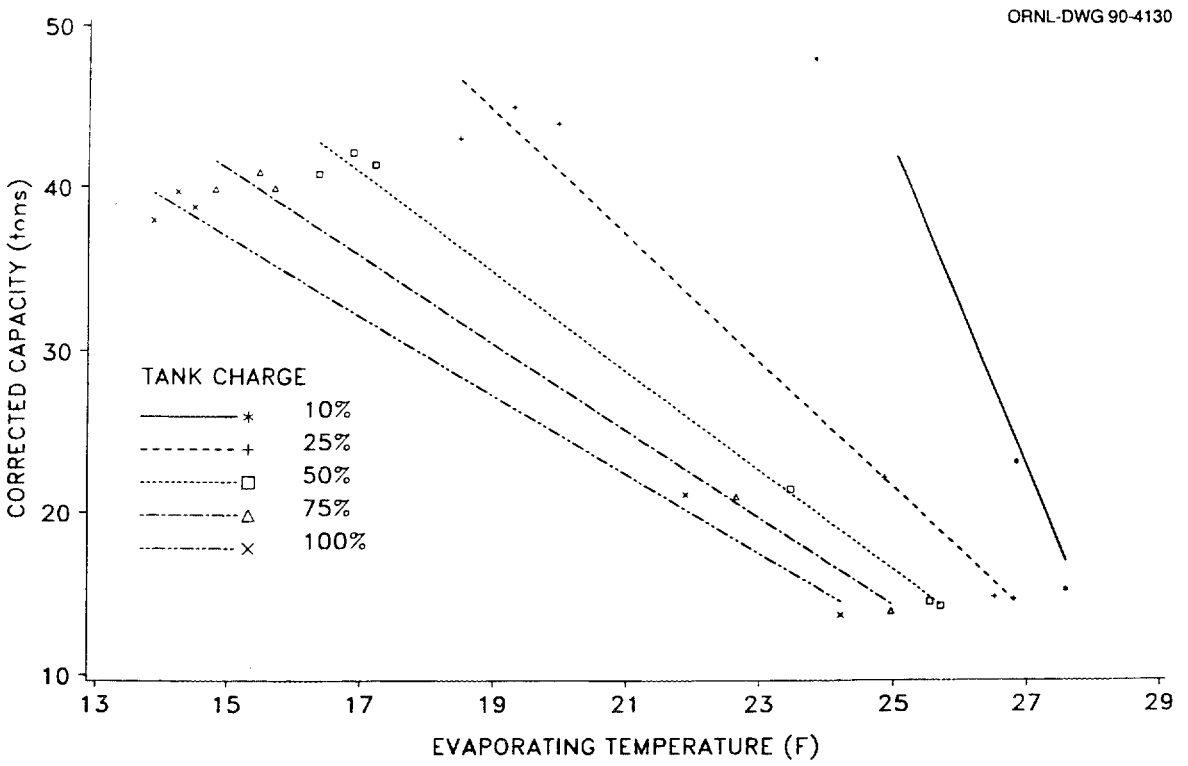

Fig. 9. Corrected capacity vs saturated suction temperature for tank charges from 10 to 100% frozen for BAC liquid-overfeed coils. All temperature measurements are $\pm 0.5°F$.

The liquid-overfeed ratio varied from this recommended value during the tests as was discussed in Sect. 3. Therefore, tank exit conditions were monitored for each test to ensure that the fluid leaving was indeed saturated by comparing the exit temperature to the saturated temperature corresponding to the exit pressure. Figure 10 is a typical example of this comparison. Aside from a few isolated points during start-up fluctuations, the fluid leaving the ice tank coils was never superheated.

Figure 11 shows the liquid-overfeed ratio calculated for each test. The lowest overfeed ratios occurred for the higher test capacities because of insufficient refrigerant inventory in the loop consisting of the tank coils and the low-pressure receiver. This problem occurred because system capacity varied widely from one test to another (on the order of 300%). This broad range in charging rate variation, while necessary in a test facility, is unlikely to occur in a commercial installation and should indeed be avoided.

The BAC coil design includes orifice plates used to ensure proper distribution of the refrigerant among the multiple coils. These orifice plates are usually sized for a specified capacity. There was some concern that excessive pressure drops would occur at the highest

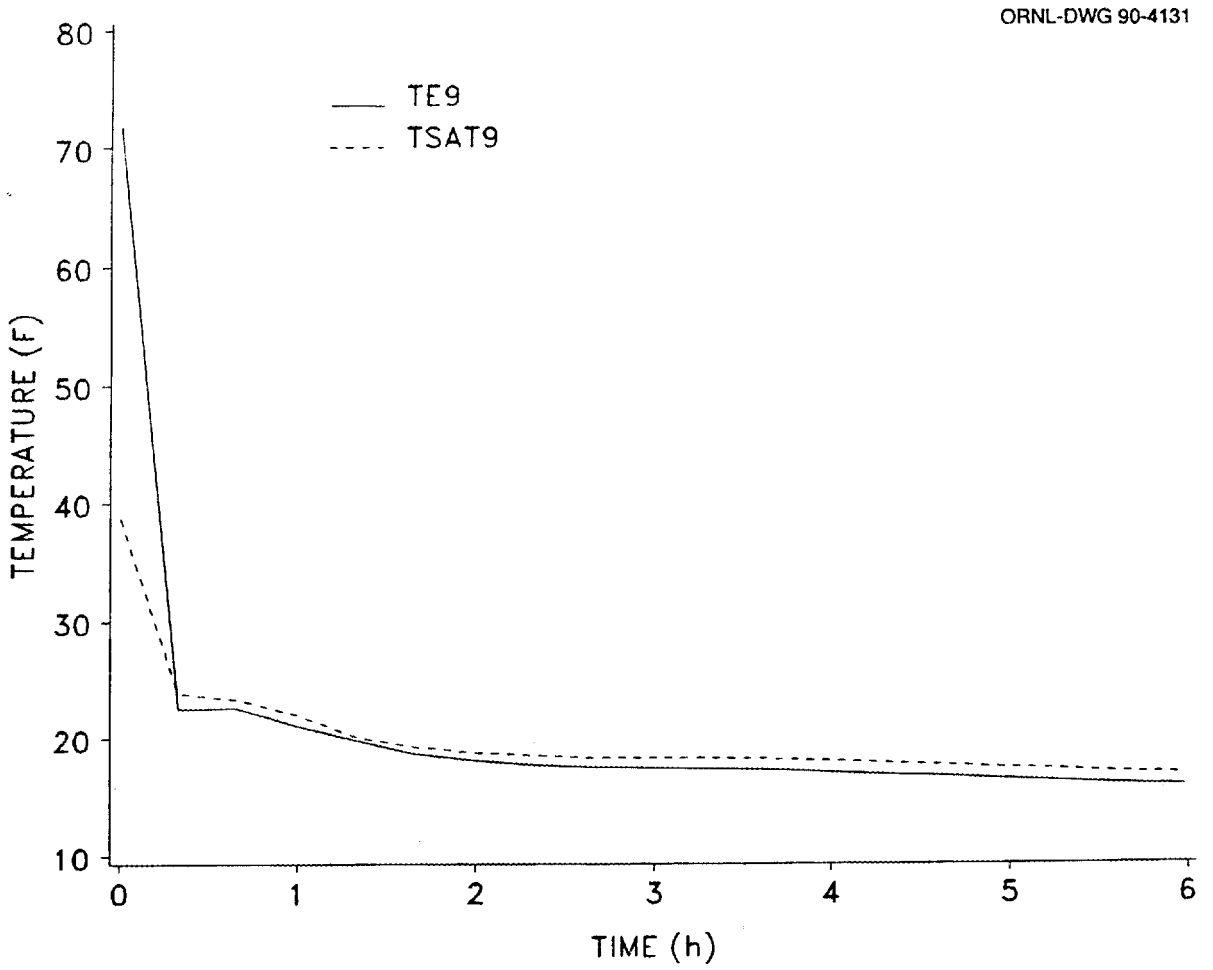

Fig. 10. Comparison of refrigerant temperature leaving liquid-overfeed coils to saturated temperature corresponding to refrigerant pressure at ice tank exit. All temperature measurements are $\pm 0.5°F$.

capacities tested because the plates had to be sized for the lowest test capacity to ensure adequate flow rates. The pressure drops, measured from the tank inlet to the tank outlet, ranged from average values of 5.8 psia at the lowest tested capacity of ~15 tons to 8.9 psia at 45 tons.

Auxiliary power requirements include the refrigerant pump and the air agitator. The average pump power was ~2 kW. If a 30-ton system was running with compressor power consumption of 1.20 kW/ton, this additional power use would increase the overall power consumption to ~1.27 kW/ton, an increase of ~6%. The agitation air compressor power use was ~1 kW. Including the tank heat gains attributable to this air source of 0.23 tons (see Sect. 4.4), for the same example system (30 tons at 1.20 kW/ton), the overall efficiency

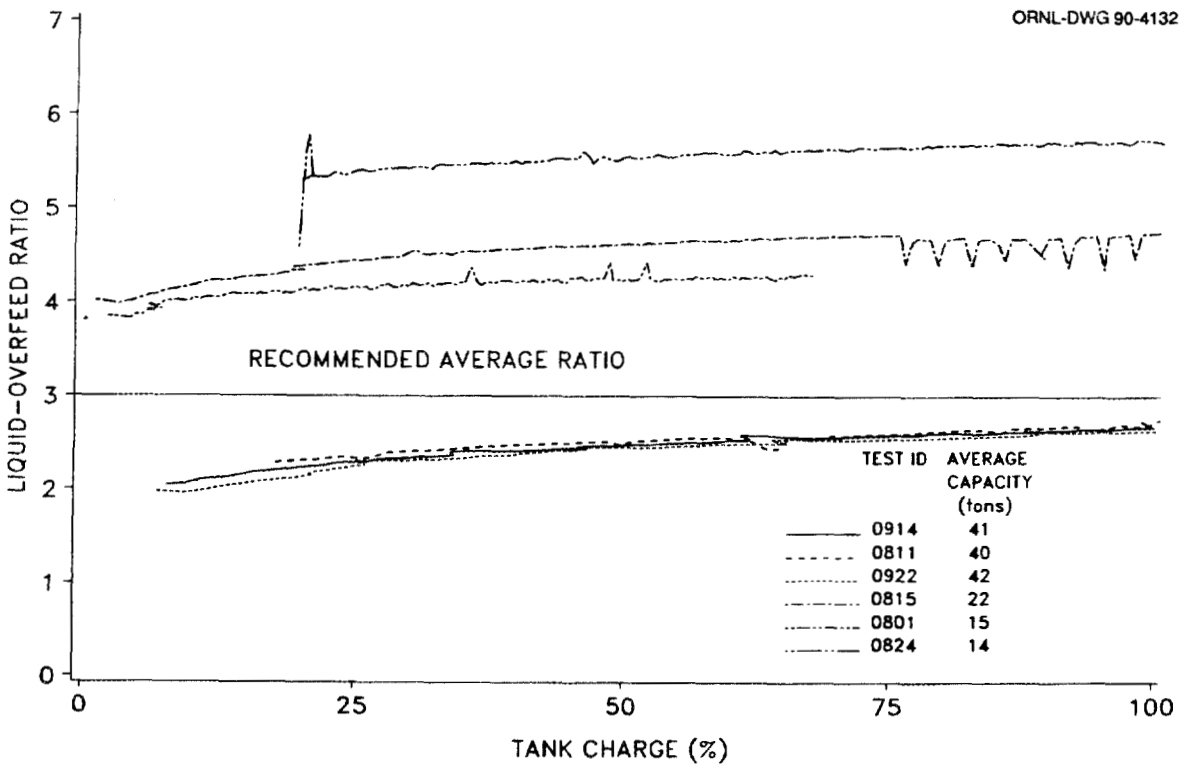

Fig. 11. Liquid-overfeed ratio summary for all liquid-overfeed charging tests.

penalty due to the agitation alone would be ~4%. The agitation air is on during ~20% of the charging cycle.

5.1.2 Brine Coils

Capacity calculations were described in Sect. 4.2.2 and are based on an energy balance on the ice tank. In comparing the calculated refrigeration capacity (based on the brine flow rate and temperature change in the ice tank) to the change in storage tank depth, the calculated value varies from values 10% low to 44% high. Based on the data values, the main contributor to this error is the temperature measurement accuracy. Because each temperature measurement is only accurate to within ±0.5°F (see Appendix A), the difference between the inlet and outlet temperatures can be off, in the worst case, by as much as 1°F. If this error bound is considered, the calculated capacity agrees with the change in tank water depth in every case. The initial tests were run at a lower brine flow rate, causing the temperature rise across the evaporator to be from 5 to 10°F and the largest expected error to be a smaller proportion of the measured capacity (from 10 to 20%). The measured error

for four of these initial tests was <5% (all on the low side), while one test was 10% low. Final tests were run at BAC's recommended brine flow rate and had temperature differences ranging from 2 to 5°F. For this temperature change, the maximum potential errors due to temperature measurement accuracy limitations range from 20 to 50%. The measured errors for these final tests were 16, 22, and 44% high. All capacity results presented here have therefore been corrected to agree with the change in tank water depth, as was described in Sect. 4.

The corrected capacity of each brine charge test is shown in Fig. 12. The tests ranged in average capacities from 14 to 33 tons. As was shown in Table 6, three of the tests — labeled 0727, 0731, and 0803 — were run at the recommended flow rate. Although the test labeled 0523 was only a partial test (it began when the ice tank was ~40% frozen), it is included for comparison to test 0803 later in this discussion.

The normalized capacity was calculated to show the decrease in capacity that occurs as ice builds up around the coils within the storage tank. All the tests shown in Fig. 13

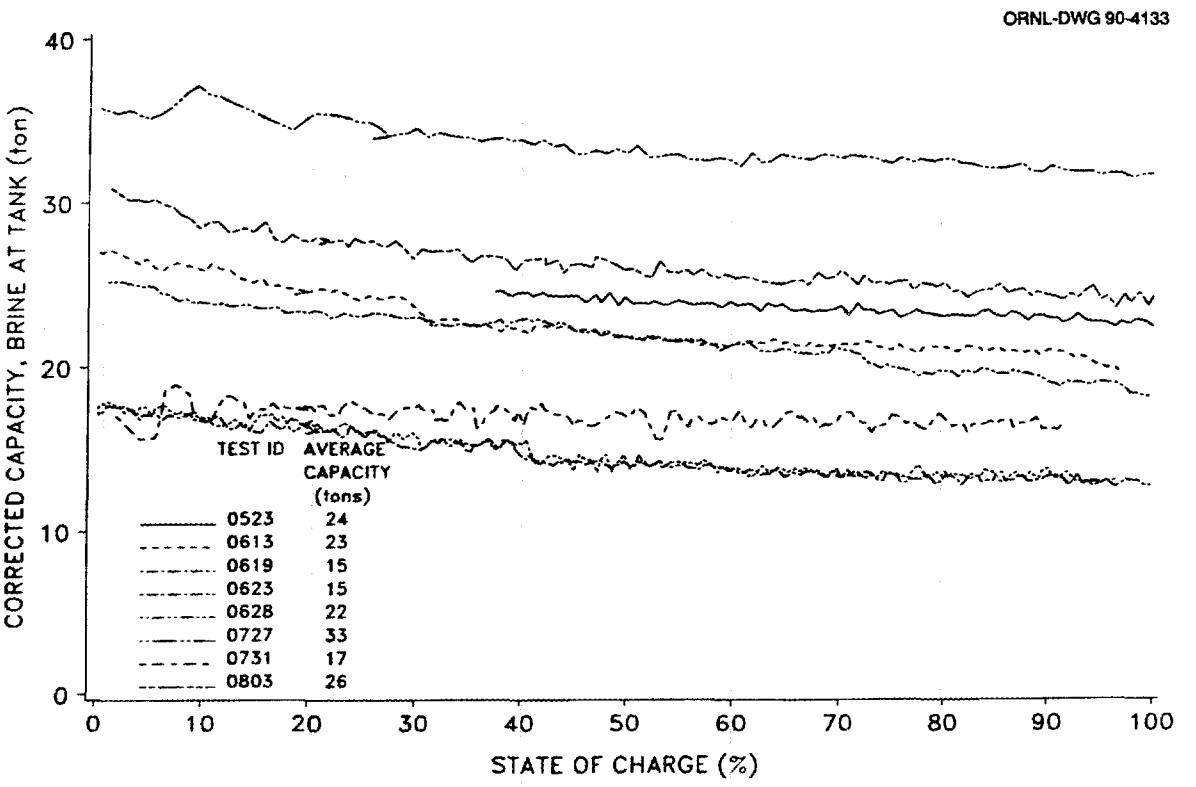

Fig. 12. Summary of BAC brine-coil tests, capacity based on brine temperature and flow measurements, corrected according to change in tank water depth. All temperature measurements are ±0.5°F.

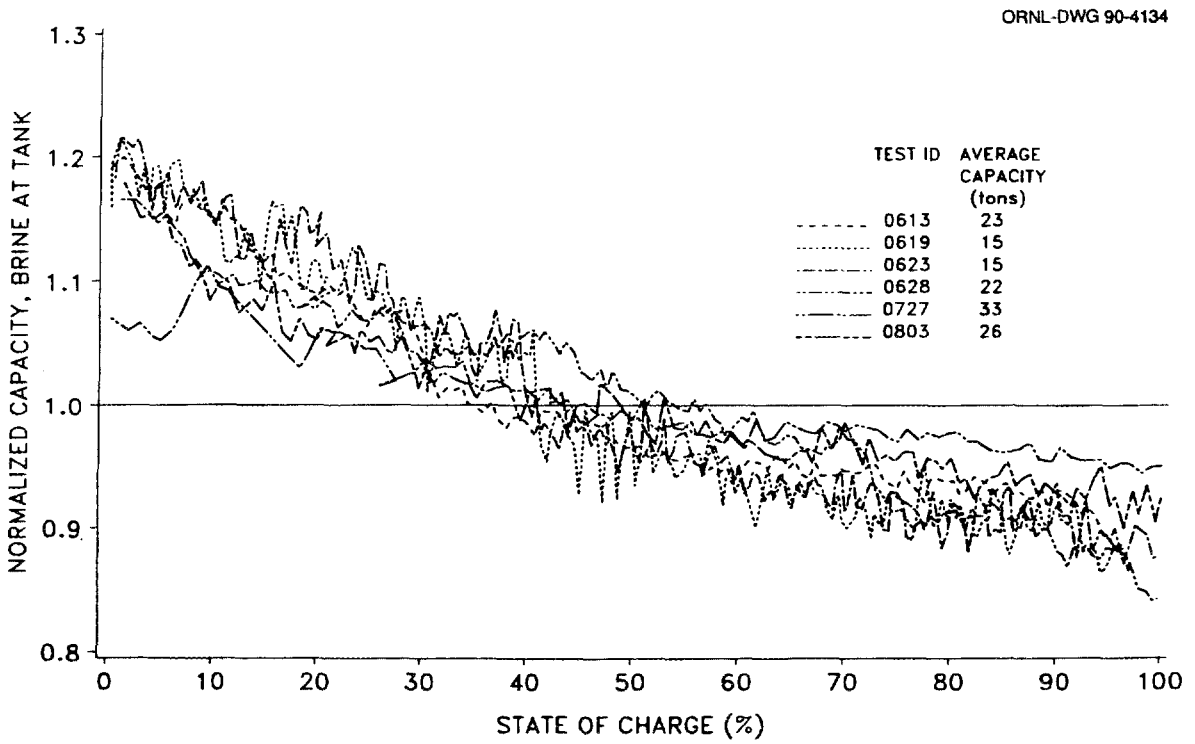

Fig. 13. Capacity of brine-coil charge tests, normalized relative to average for each test.

extended from essentially 0 to 100% charged, and no mathematical models were used. There does not appear to be any clear trend in the shape of the normalized capacity curves as the average capacity increases, as there was for the liquid-overfeed tests. Because the roughness introduced by the capacity fluctuations makes this plot difficult to read, mathematical models of the capacity were used to generate smoother normalized capacity curves as shown in Fig. 14. The models for a few of the tests were statistically unacceptable, and those tests have not been included in this figure. The curves shown are all based on models with adjusted squared correlation coefficients >0.96. The T-test results for the parameter estimates were >0.99 for all estimates. Given the good model correlations, it is reasonable to use Fig. 14 to evaluate the limits of the normalized capacity as well as the crossover point at which the capacity drops below the average value. All the tests seem to start at a capacity ~20% greater than the test's average capacity, and all seem to reach the average when the tank is ~45% charged. The only test at BAC's recommended flow rate included in Fig. 14 is test 0803. This test shows a somewhat shallower slope and a lesser amount of capacity derating as the test reaches the 100% mark. As was anticipated from Fig. 13, the average capacity, or charging time, appears to have little effect on the amount of derating or the shape of the normalized capacity curve.

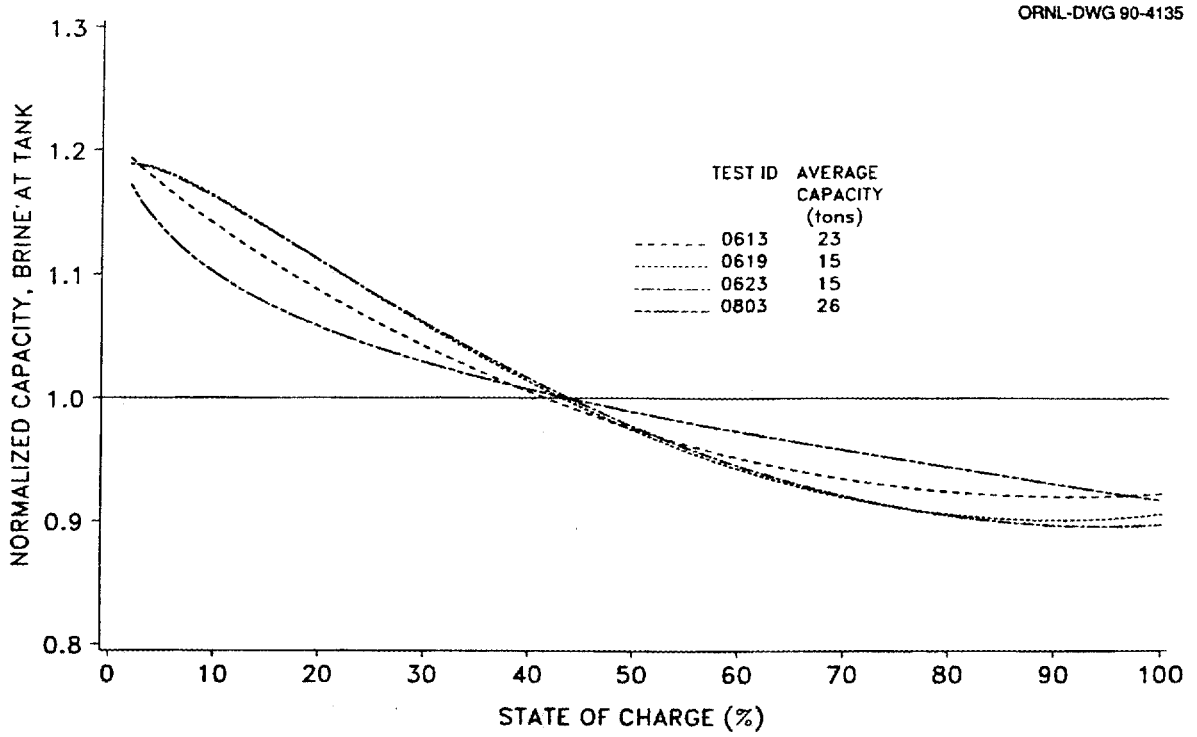

Fig. 14. Capacity of brine-coil charge tests, generated by test-specific mathematical models of capacity as function of tank charge, normalized relative to average for each test.

The decrease in capacity during a charge cycle is caused by the reduction in saturated suction temperature at the compressor. This reduction is caused by the increased thermal resistance of the ice layer building on the heat exchanger tubes, which causes lower brine temperatures in the evaporator/chiller. The temperature of the brine entering the ice tank is shown in Fig. 15. (The accuracy of the temperature measurements is $\pm 0.5°F$, as is discussed in Appendix A.) As expected, the tests that were run at a higher capacity show the lowest brine temperatures. However, the brine flow rate is also an important parameter in determining the brine temperature. As mentioned before, tests 0731, 0803, and 0727 were run at BAC's recommended brine flow rate. The effect of brine flow rate on brine temperature is most readily examined by comparing tests 0523 and 0803. These tests were run at very similar charge rates as was shown in Fig. 12. Test 0803, at the higher flow rate, shows brine temperatures 4°F higher than the comparable test at the lower flow rate.

The cumulative capacity is shown in Fig. 16. This plot shows that, just as for the liquid-overfeed coils, there was no difficulty in fully charging the storage system under a wide range of charging rates. Those tests that are shown stopping slightly short of a full charge were stopped by a programmed timer, not by any difficulty in the ice storage system. Tests 0523 and 0731 are not shown on this plot because they were only partial tests.

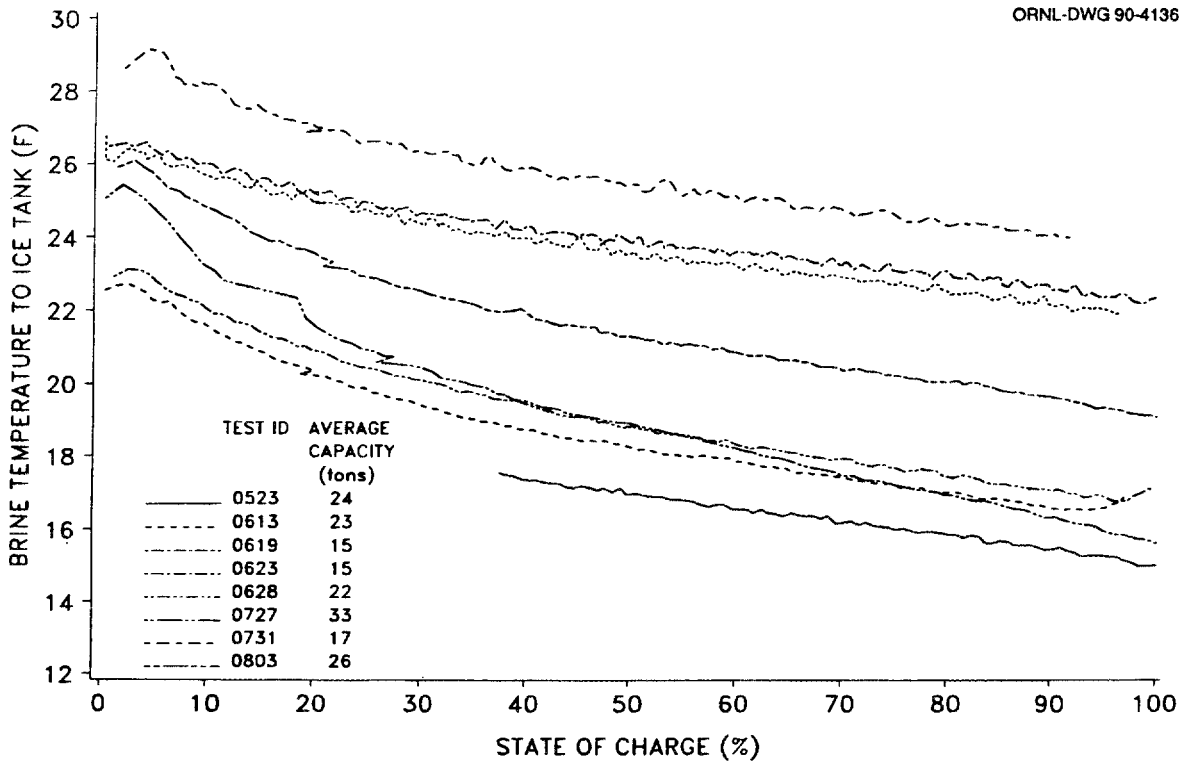

Fig. 15. Summary of tank brine inlet temperature profiles for all brine-coil charge tests. All temperature measurements are ±0.5°F.

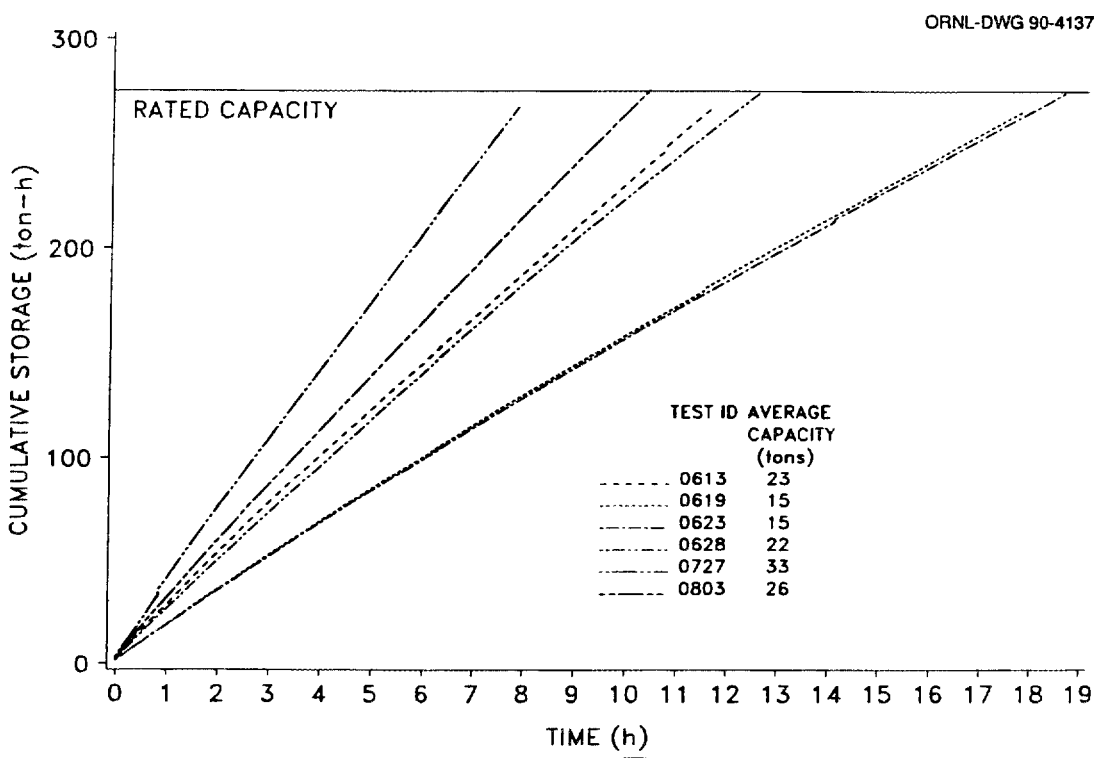

Fig. 16. Summary of cumulative energy storage in ice tank for BAC brine-coil tests.

To aid customers in selecting the proper chiller, BAC provides the time-weighted average brine temperature to and from the ice tank during charge cycles of varying durations. The brine coils for the TSU-275B were redesigned after their latest technical bulletin was printed,[1] so reference values of average inlet and outlet brine temperatures was not available. However, for all of their brine coils, the time-weighted average of the brine inlet and outlet temperatures is dependent only upon the build time. These are shown in Fig. 17, along with the comparable values measured during the tests. The average brine temperature for those tests run at BAC's recommended brine flow rate of 135 gal/min were slightly higher than those quoted in the BAC literature, so the BAC numbers are conservative. Also shown on Fig. 17 are the time-weighted average of the brine inlet and outlet temperatures measured during the tests. Due to the complexity of any given ice storage application, BAC also runs an in-house computer model for each customer. A comparison of the model predictions to test results is discussed in Appendix B.

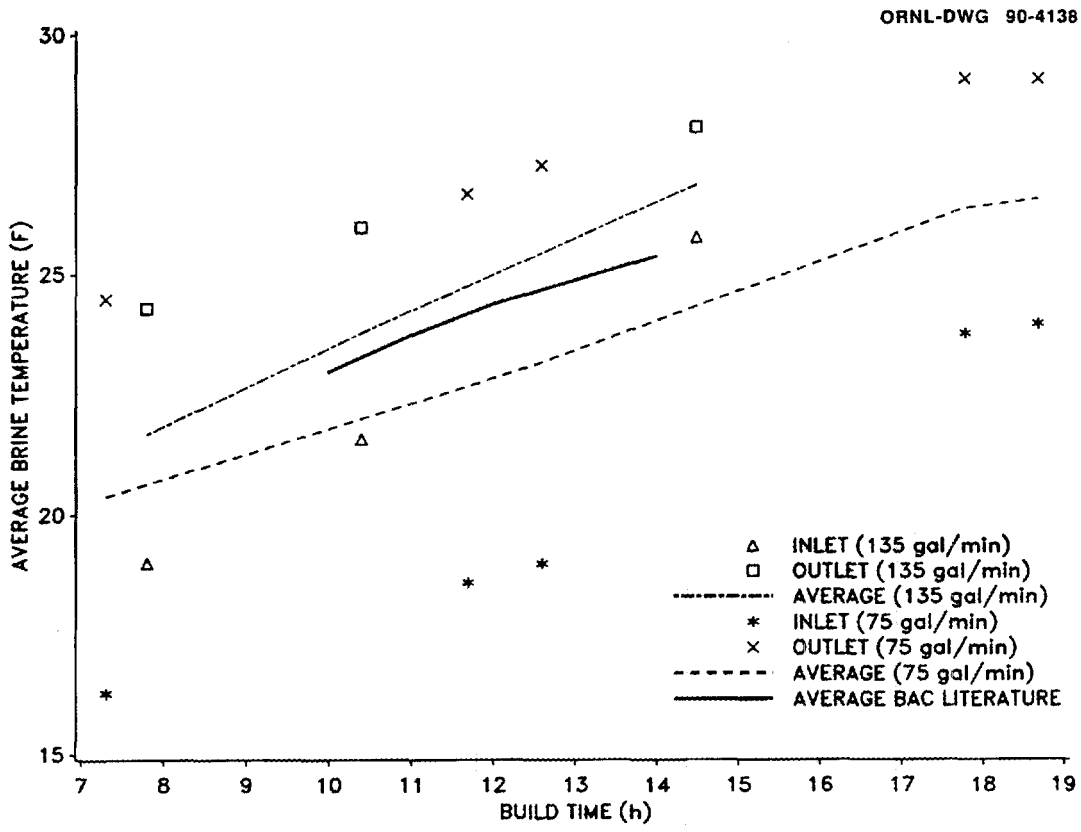

Fig. 17. Time-weighted average brine temperatures vs ice build time for BAC brine coils. All temperature measurements are $\pm 0.5°F$.

Traditional compressor curves, when used with chiller/evaporator data, provide adequate guidance when selecting equipment for constant temperature systems, such as air conditioners, but are less useful for ice storage systems. The test data were therefore analyzed with the aim of aiding system designers in predicting system performance with variable load temperatures. The test data were correlated with tank state-of-charge (relative to the rated full charge). The latent tank charge was chosen so that the results could be used for tanks of similar design but with different storage capacities.

While Fig. 17 showed the brine temperatures averaged over the entire charging period, Figs. 18 and 19 show the system capacity vs brine inlet temperature for the ice tank at 10, 25, 50, 75, and 100% charge for the two brine flow rates tested, 135 and 75 gal/min, respectively. Figure 18 represents the manufacturer's recommended flow rate. The tank state of charge is based on the measured change in tank water depth. The lines shown are linear regressions based on the data points. As expected, the linear regressions show very strong

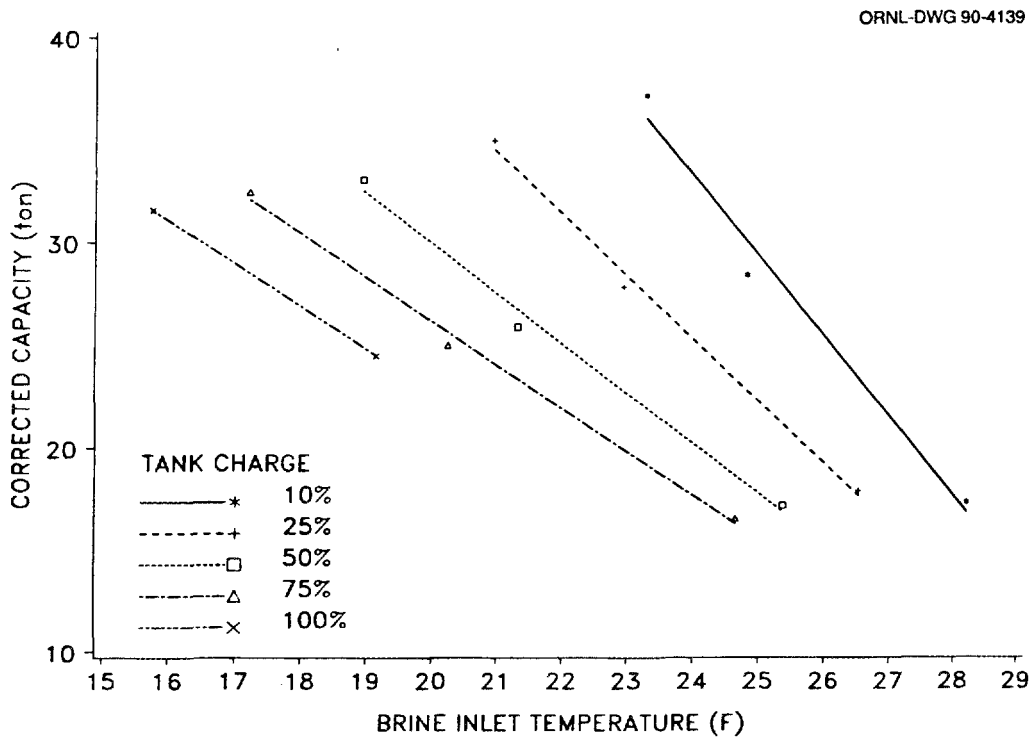

Fig. 18. Corrected capacity vs storage tank brine inlet temperature for tank charges from 10 to 100% frozen for BAC brine coils at a brine flow rate of 135 gal/min. All temperature measurements are $\pm 0.5°F$.

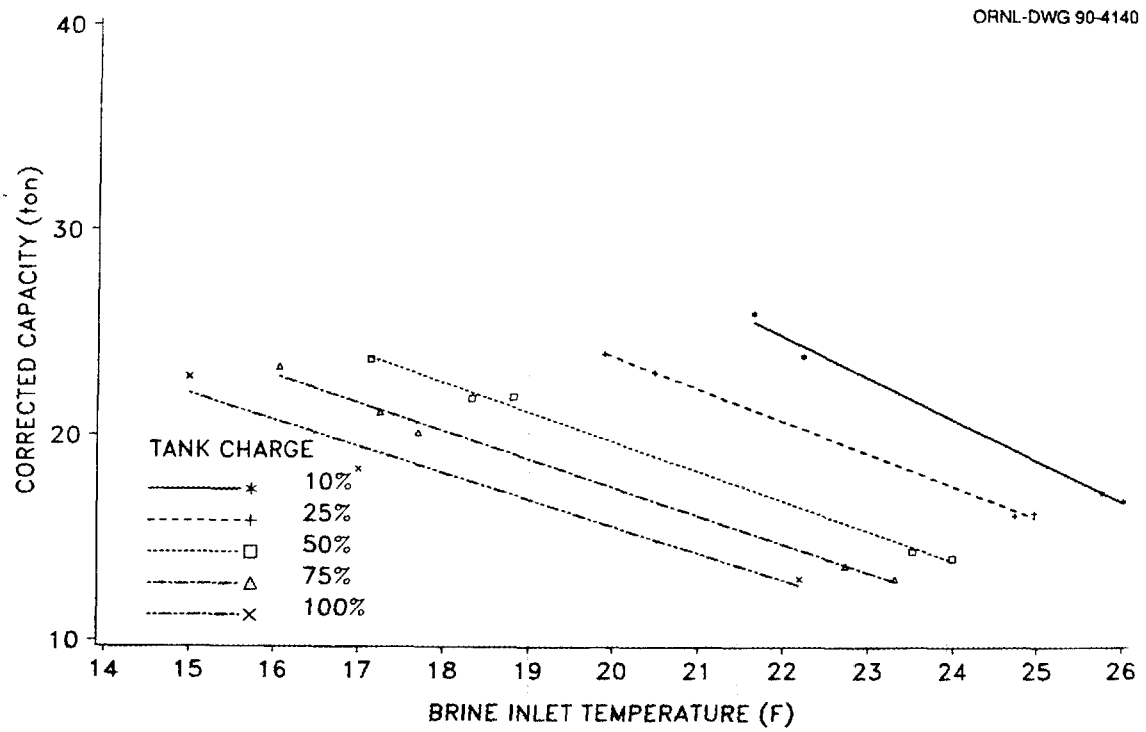

Fig. 19. Corrected capacity vs storage tank brine inlet temperature for tank charges from 10 to 100% frozen for BAC brine coils at a brine flow rate of 75 gal/min. All temperature measurements are ±0.5°F.

adjusted squared correlation coefficients, the lowest value being 0.96, with 7 out of 10 being greater then 0.99. (The regression for 100% frozen with the higher flow rate has no regression coefficient because there are only two data points.) This figure can therefore be used to assess the range of operating conditions that the chiller/evaporator and compressor must experience during a charge cycle.

Auxiliary power requirements include the brine pump(s) and the air agitator. The pressure drop through the brine coils was not measured. The average pump power was about 1 kW at the 75-gal/min flow rate and ~4 kW at the 135-gal/min flow rate. If a 30-ton system was running at the higher flow rate with a compressor power consumption of 1.2 kW/ton, this additional power use and heat addition would increase overall power consumption to ~1.4 kW/ton, an increase of ~15%. The agitation air compressor power use was ~1 kW. Including the tank heat gains attributable to this air source of 0.23 tons (see Sect. 4.4), for the same example system (30 tons at 1.2 kW/ton), the overall efficiency penalty due to the agitation would be ~4%. The agitation is on during about 20% of the charging cycle.

5.2 DISCHARGE PERFORMANCE

The discharge tests were summarized in Table 7. Each of these tests was run until the ice was completely melted. (Later, modifications were made to the test procedure that call for a discharge test to end when the desired heater outlet temperature can no longer be maintained. This improved procedure tests the storage system's ability to consistently deliver the rated capacity after a series of full and partial discharges, revealing problems that may be caused by uneven ice melting and/or ice buildup. However, this aspect of ice storage operation was not tested on the BAC unit.) The results presented here are based on test data up until the tank outlet temperature reached 44°F. Later in this section, the effect of maximum acceptable outlet temperature on the total available capacity is discussed.

As mentioned in Sect. 4.3, the discharge capacity was measured in four different ways. Figure 20 shows the relative consistency of these different values in revealing the cumulative cool storage harvested from the ice tank. The heater energy measurements are always low

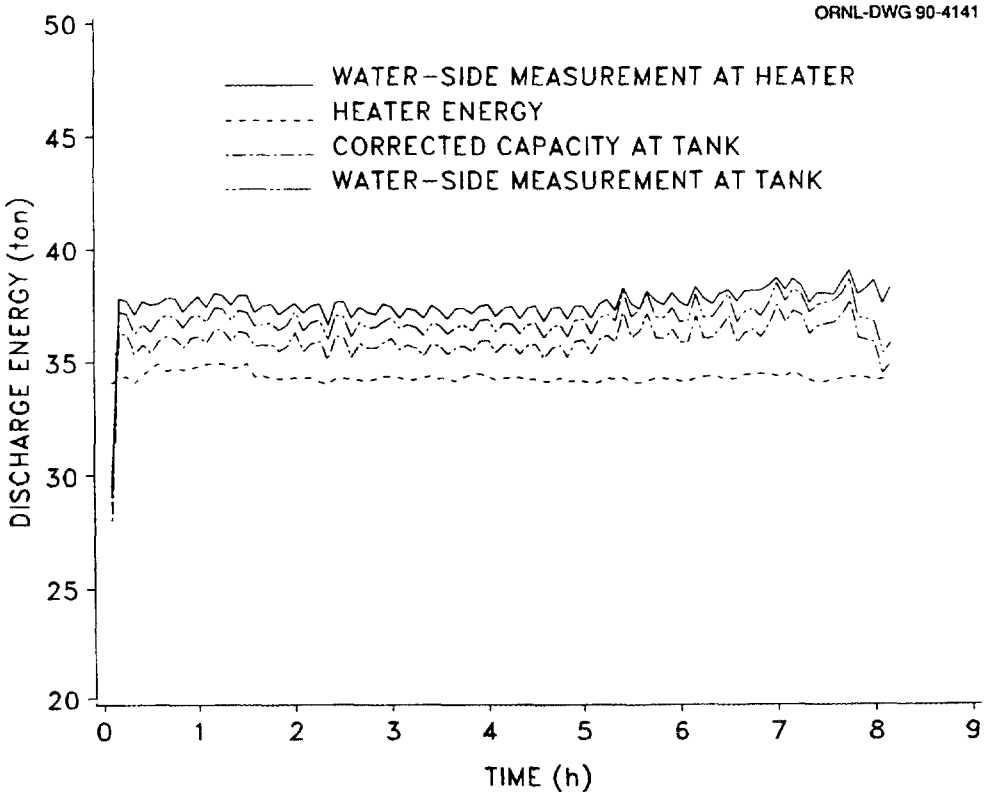

Fig. 20. Comparison of discharge energy as measured at four different locations from test run on May 24, 1989.

because of losses in the electrical controller used to select the heater power level. The water-side measurement at the heater should be slightly less than the water-side measurement at the tank because of heat gains by the circulation pumps. However, temperature measurement errors of ±0.5°F can occur at any of the four monitoring points used to calculate the change in water temperature across the tank and heater. Therefore, the measured discharge energy at the tank was corrected to match the measured change in tank cool storage inventory. This inventory included both the amount of ice melted and the rise in the mixed temperature of the tank's water. This corrected value is also shown in Fig. 20.

This corrected value is used in Fig. 21 to present the discharge energy for all the tests. The latent state of charge is based on the water depth in the tank and does not account for the sensible gains in the water in the tank. The tests therefore appear to end before the latent capacity has been fully utilized. However, the cooling energy available up to a tank outlet temperature of 44°F consistently meets and exceeds the tank's rated capacity

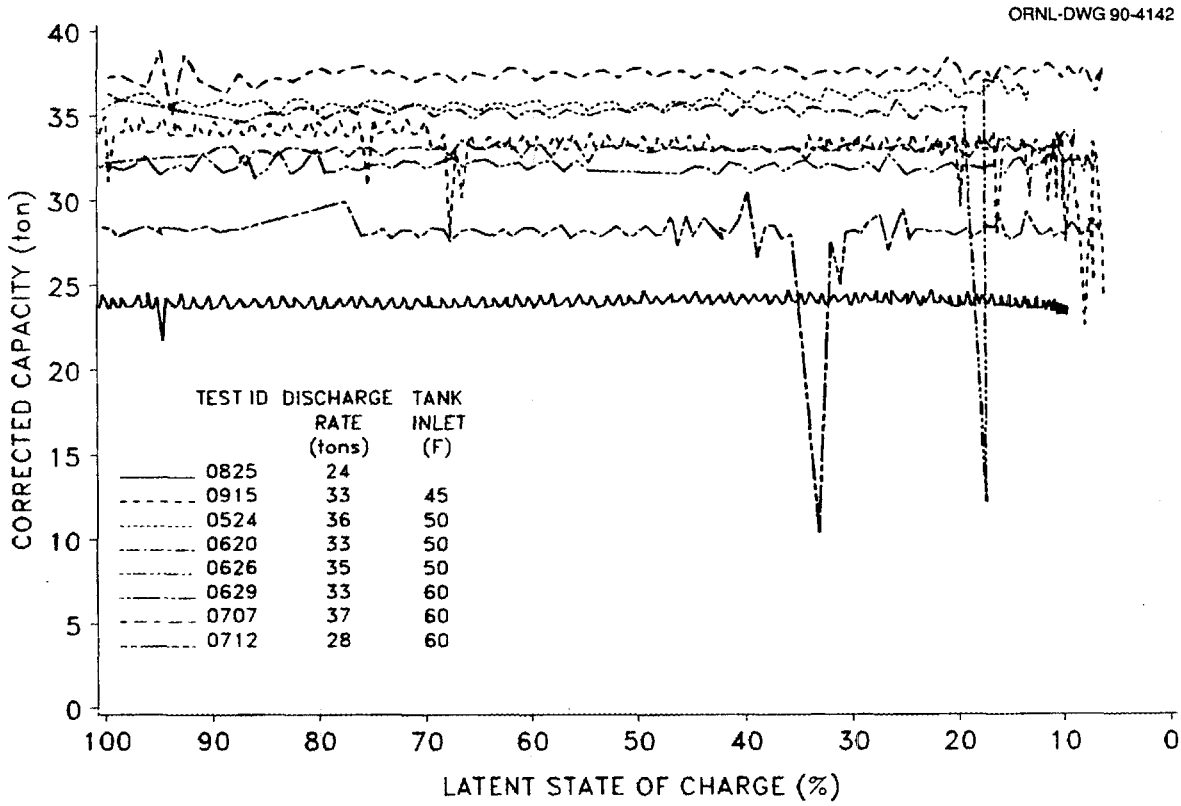

Fig. 21. Corrected discharge energy vs latent state of charge, or ice inventory, as measured by tank water depth. Data end when water temperature leaving ice tank exceeds 44°F. All temperature measurements are ±0.5°F.

of 275 ton-h (266 ton-h for the liquid-overfeed coils) (see Fig. 22). The flat steplike breaks in the lines are caused by tests that took place over 2 d with a long shutdown period. During this time, the water in the piping (~120 gal) returns to room temperature and places an additional instantaneous load on the system when the test is restarted. This step also includes standby heat gains to the tank during the shutdown period. Thermodynamically, the ice remaining at the end of the discharge tests would be consumed returning the water inventory to 32°F before the start of the next charge cycle. Whether this melting would actually occur was not tested because the heater power and water circulation were maintained for each test until all the ice was melted.

The water temperature leaving the ice tank maintained a constant temperature between 33 and 34°F during most of the tests, as is shown in Figs. 23 and 24.

The water temperature tends to rise after ~80% of the latent heat has been removed. The temperature rise becomes steeper after all the latent energy has been used. Tests were

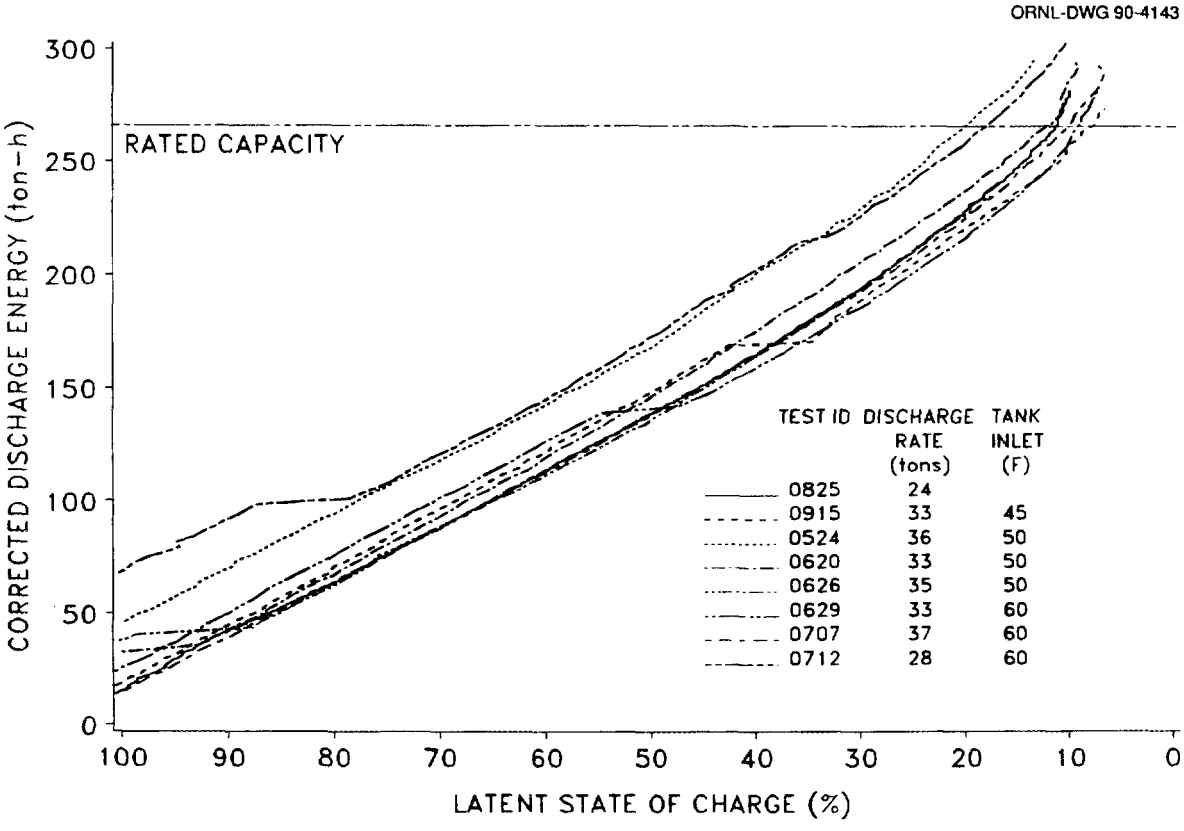

Fig. 22. Cumulative corrected discharge energy summary for all BAC discharge tests, ending when water temperature leaving ice tank exceeds 44°F (horizontal reference line at rated tank capacity of 266 ton-h). All temperature measurements are ±0.5°F.

ORNL-DWG 90-4144

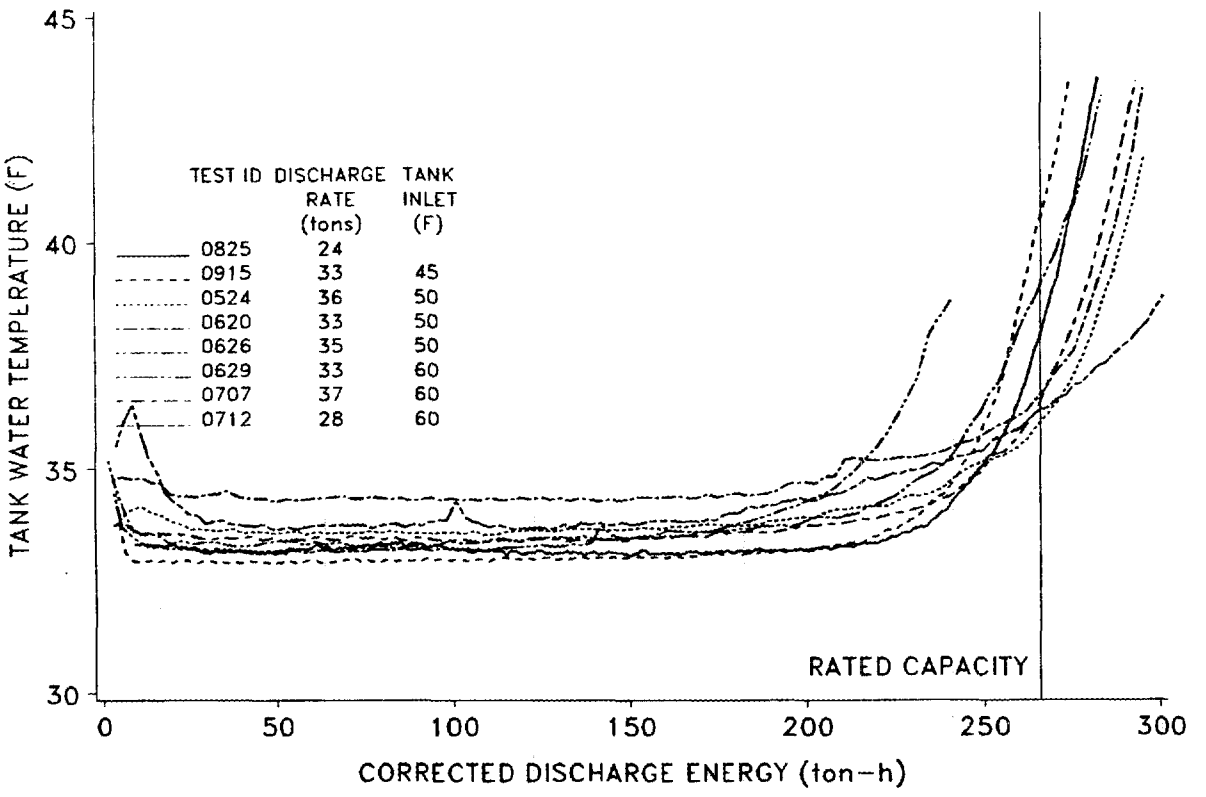

Fig. 23. BAC discharge test summary: tank water outlet temperature vs corrected cumulative discharge energy, reference line at 266 ton-h. All temperature measurements are ±0.5°F.

run with heater outlet (tank inlet) temperatures between 45 and 60°F. The tank inlet temperature did not appear to have any measurable effect on the tank outlet temperature.

There was some concern that the temperature measurement at the ice tank outlet was imprecise. Indeed, after one test, not reported here, showed abnormally high tank outlet temperatures, the RTD was retested and replaced. Therefore, for all the tests, an additional check on the tank outlet temperature was made based on an energy balance at the mixing point located at the heater outlet. Assuming that the heater inlet and outlet temperatures and the measured flows were correct, the calculated tank outlet temperature agreed with the measured tank outlet temperature for five out of the reported eight tests. However, for test 0620, the measured temperature was 0.8°F higher than the calculated value. Test 0629 showed a measured temperature that was 1.3°F lower than the calculated value. Test 0712 had a measured temperature that was 0.6°F low during the beginning of the test, but agreed well during the latter portion.

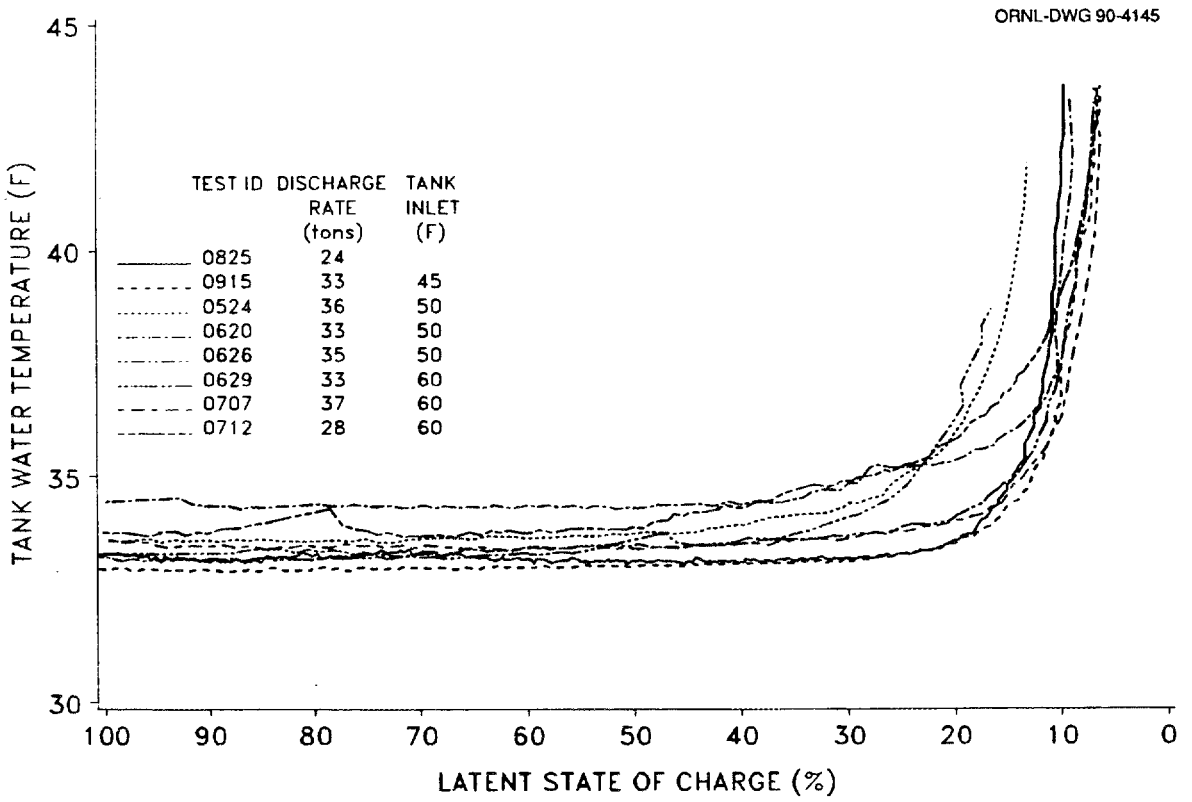

Fig. 24. BAC discharge test summary: tank water outlet temperature vs tank state-of-charge. All temperature measurements are ±0.5°F.

Figure 25 can be used to predict the capacity available for several specified maximum tank outlet temperatures over a range of discharge periods or rates. These lines show that the cool storage available from the BAC ice tank is relatively insensitive to both discharge rate and maximum tank outlet temperature. This insensitivity is caused by the relatively constant temperature of the water leaving the BAC tank throughout most of the discharge cycle. The temperature profile of the BAC tank outlet water was also unaffected by changes in the tank inlet temperature from 50 to 60°F. Based on these tests and the results presented in Figs. 22–25, a storage tank sized solely according to the latent ice storage capacity (including adequate allowances for standby losses) is capable of providing a relatively constant temperature to the load throughout most of the discharge cycle.

Power requirements during discharge include both water pumping power and agitation air compressor power. The agitation air compressor uses ~1 kW and causes heat gains to the tank at a rate of ~0.23 tons. The water pumping power varies with the water flow rate and ranged from 0.4 to 1.1 kW (see Fig. 26).

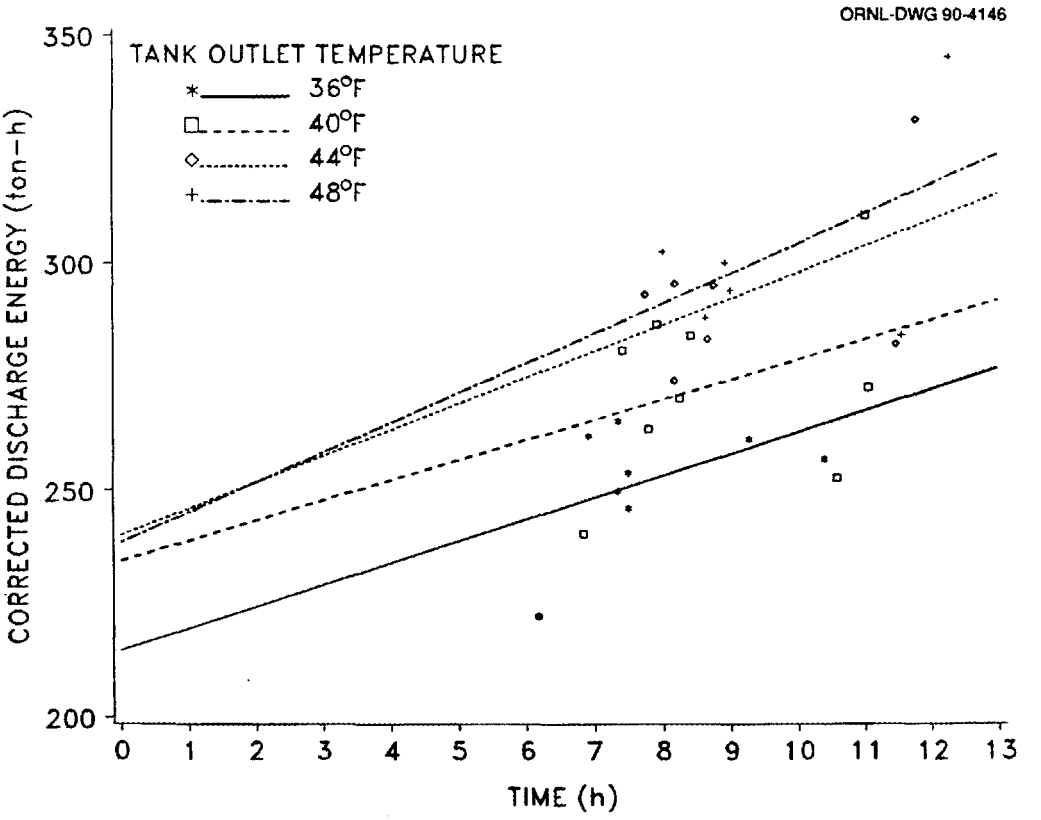

Fig. 25. BAC discharge test summary: cumulative discharge energy available for maximum tank outlet temperatures of 36, 40, 44, and 48°F for different discharge periods. All temperature measurements are ±0.5°F.

Several tests were run at conditions outside the normal operating range. Three of these are shown in Figs. 27–29, labeled 0913, 0608, and 0712. Test 0825, a proper discharge test, is shown on these figures to enable comparison to a more normal discharge temperature profile.

Before test 0913 began, the tank was overcharged by ~25%, and the ice was partially bridged between the coils in both the vertical and horizontal directions. Under this condition, the air agitation was less effective in mixing the water in the tank. Also, the air agitation was not turned on immediately during this test, as can be seen by the sharp spike where the temperature reaches ~42°F near the beginning of the test. After the agitation air was turned on, the temperature for this case dropped to around 36°F and remained there until the ice was ~70% melted.

Test 0712 also started with an overfrozen tank and shows a more moderate increase in outlet temperature during the discharge period. These two tests show that it is important

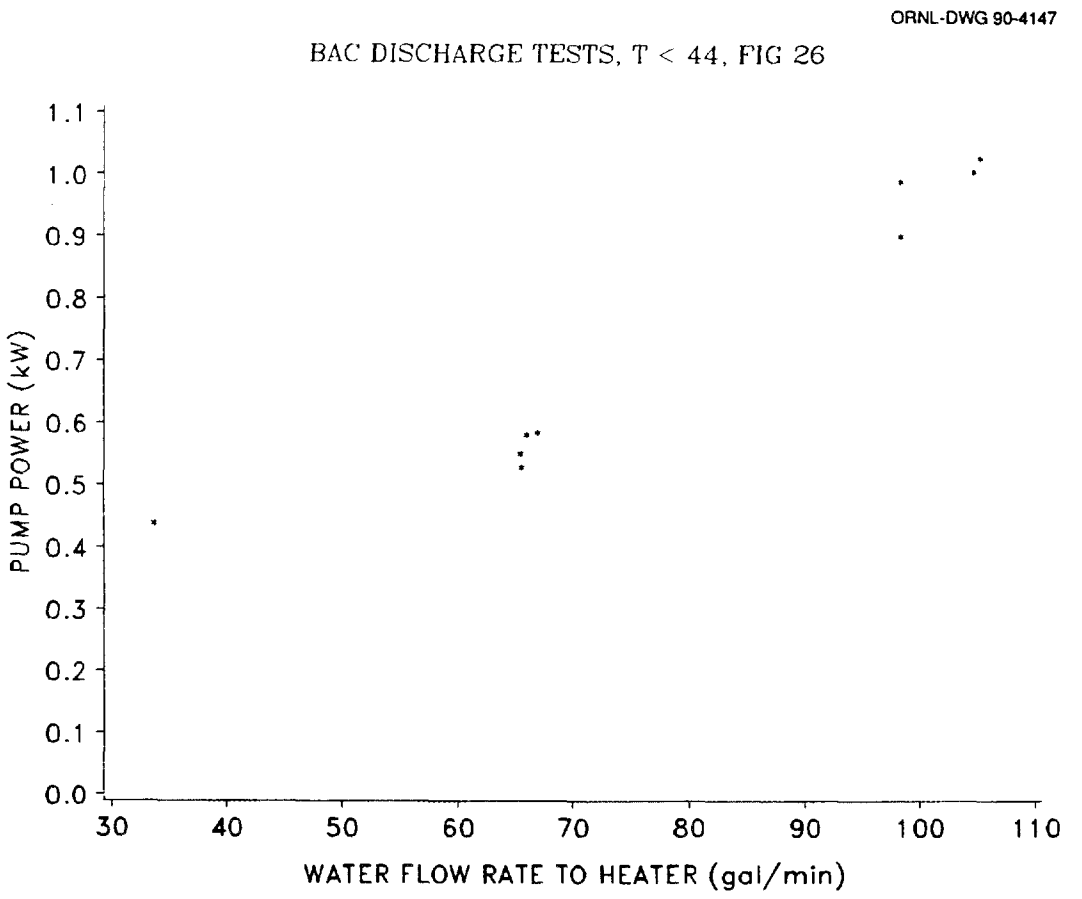

Fig. 26. Average pump power required for BAC discharge tests.

to avoid overcharging the ice tank. However, they also demonstrate that the consequences of such an operational error would not prevent the delivery of adequate cooling under most conditions. Figures 28 and 30 show the discharge energy from each of these tests until the tank outlet temperature reached 44°F. Except for test 0608, each test provided more than the rated cooling capacity.

Test 0608 started with a properly charged tank, but the air agitation was not turned on for the first 4 h of the test, producing an elevated tank outlet temperature. Once the air agitation was turned on for this test, the temperature dropped to ~34°F, still slightly higher than would be expected if the agitation had been on during the entire test. (The air agitation has an effect on the tank height, which is used to measure the state of charge. This accounts for the difference in the temperature profile of Fig. 27 compared to Fig. 28 at the point where the agitation is first turned on.) This test provided slightly less than the rated amount of cooling at temperatures <44°F. Proper air agitation, as recommended by the manufacturer, is therefore vital to effective discharge of this storage system.

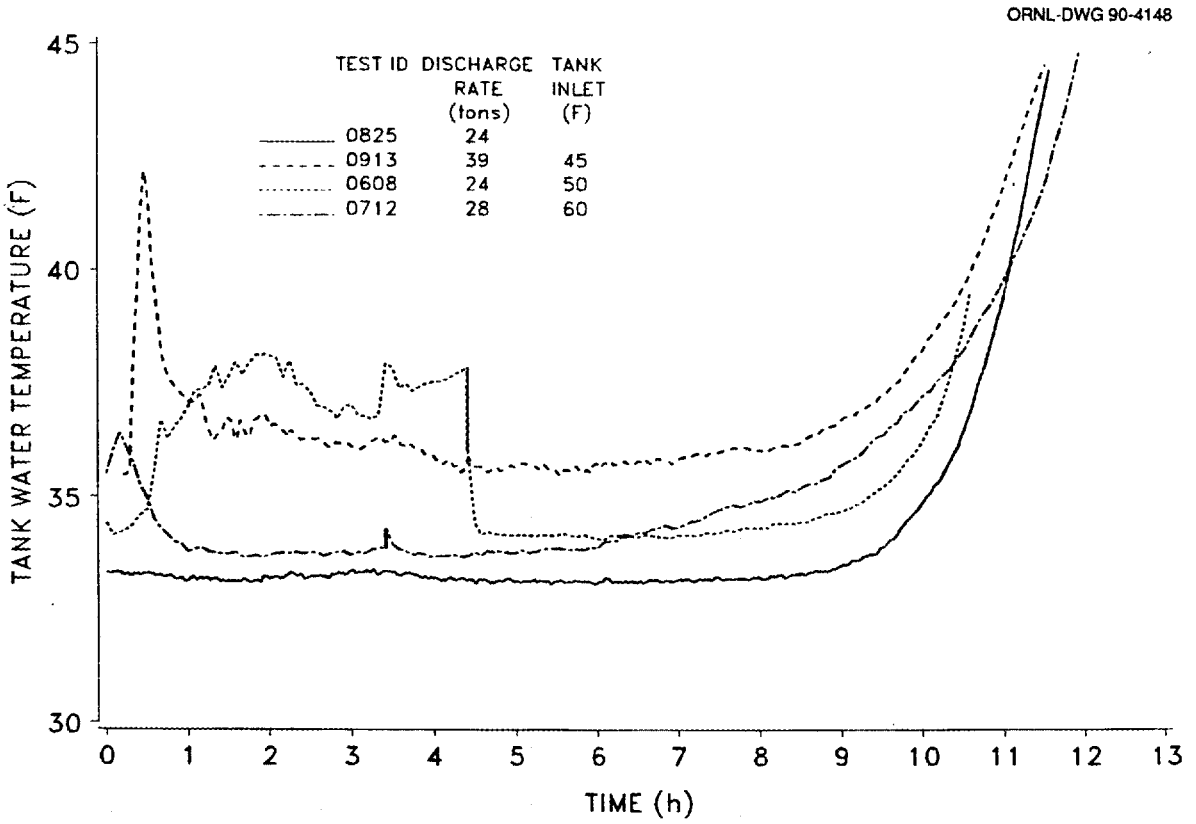

Fig. 27. BAC discharge tests at conditions beyond the normal operating range: tank water outlet temperature vs time. All temperature measurements are ±0.5°F.

5.3 STANDBY HEAT GAINS

Standby heat gains were measured in tests with the tank charged with ice and in tests with the tank charged with chilled water. The change in tank depth, with the measured ice density of 57.2 lb/ft^2 and an ice heat of fusion of 144 Btu/lb, gave the latent heat gain for a tank containing ice. The change in tank water temperature, based on a tank inventory of 4330 gal of water, yielded a heat gain of 3.01 ton-h/°F rise.

Over nine tests ranging in length from 16 to 69 h, the average (weighted according to test duration) heat gain rate was 0.6 tons. Three of the tests were longer than 63 h in duration. These tests should give a more accurate reading on standby losses than shorter tests. The average recorded gain rate for these tests was 0.4 tons. Based on the rated capacity of 266 ton-h, this loss rate can be expressed as 0.002 ton/ton-h, or alternatively, it would take 665 h (28 d) for a fully charged tank to melt.

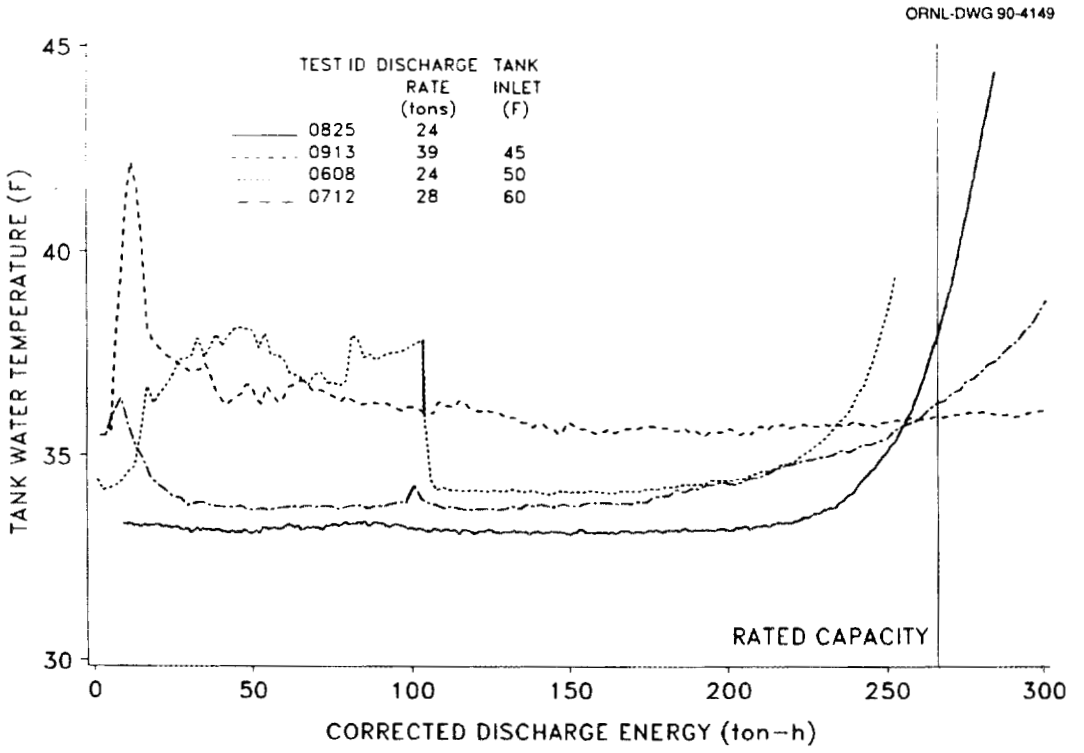

Fig. 28. BAC discharge tests at conditions beyond normal operating range: tank water outlet temperature vs corrected cumulative discharge energy, reference line at 266 ton-h. All temperature measurements are ±0.5°F.

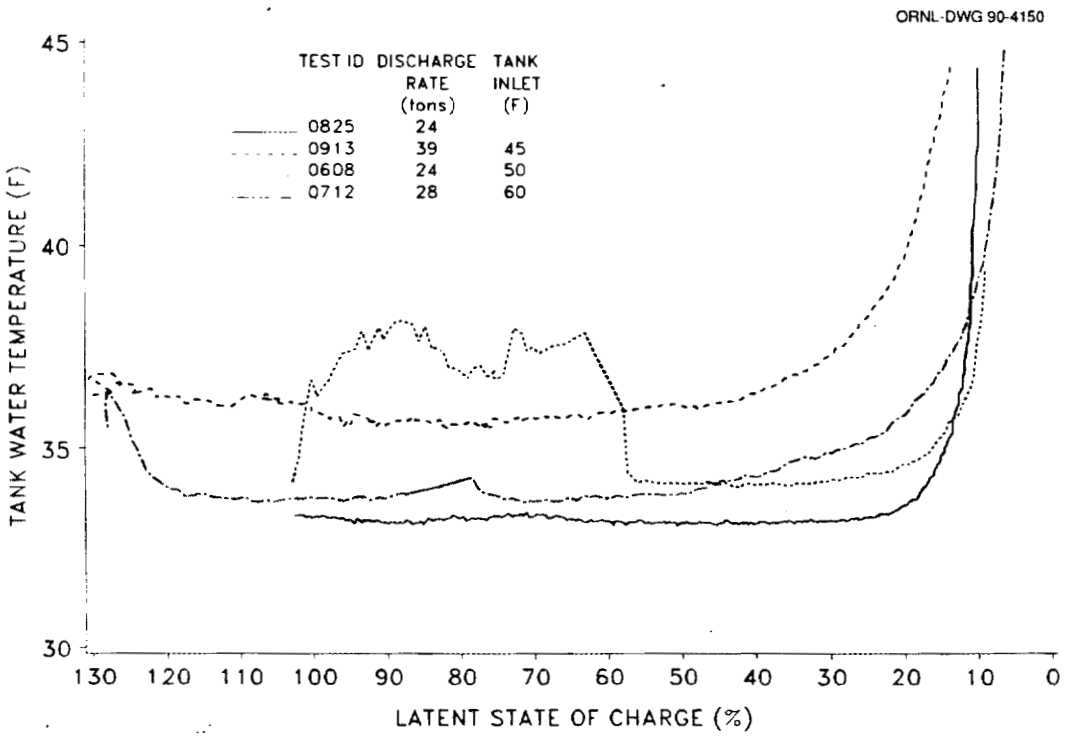

Fig. 29. BAC discharge tests at conditions beyond normal operating range: tank water outlet temperature vs tank latent state of charge. All temperature measurements are ±0.5°F.

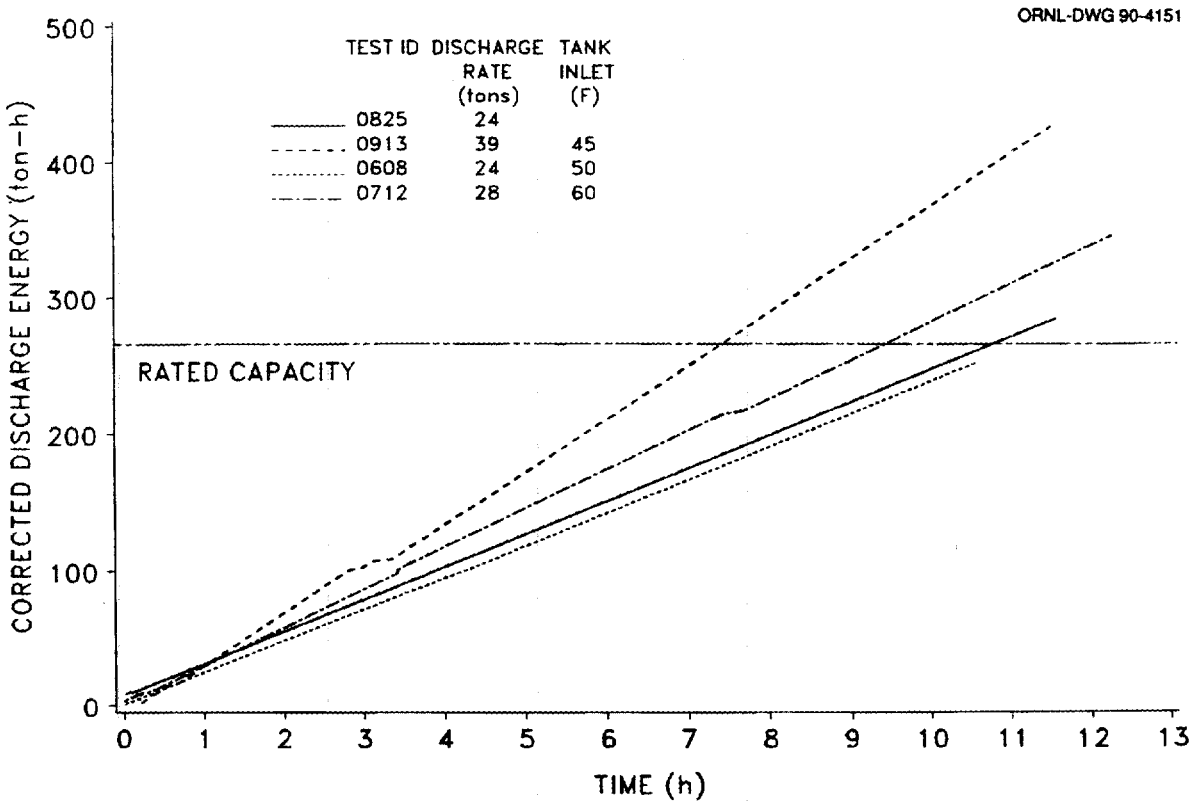

Fig. 30. Cumulative corrected discharge energy summary for BAC discharge tests at conditions beyond normal operating range; data end when water temperature leaving ice tank exceeds 44°F (horizontal reference line at rated tank capacity of 266 ton-h). All temperature measurements are ±0.5°F.

The ambient temperature was relatively constant during the standby tests at ~80°F. The test facility is in a sheltered indoor location, so there were no solar gains. The shell area of the tested tank was ~580 ft^2. For the heat gain rate of 0.4 tons, the average tank U-value is 0.17 Btu/ft^2-°F (corresponding to an R-value of about 6). BAC literature describes sidewall insulation of R-13 and top and bottom insulation of R-8. The discrepancy in predicted and measured heat gains could be caused by a small amount of air leakage around the top access plates. Any such air leakage would lead to latent heat gains because of water condensation. For example, a water condensation rate of 0.33 gal/h would correspond to a heat gain of 0.25 tons. During a 10-h charge, this increased volume of 3 gal would cause a 0.04-in. change in tank height, only ~1% of the total change in tank height measured during a typical charge cycle.

6. CONCLUSIONS AND RECOMMENDATIONS

The BAC ice storage system tested was consistently able to store and discharge the rated capacity of 266 ton-h (275 ton-h for the brine coils) for a wide range of charging rates, brine flow rates, and liquid-overfeed ratios. The average evaporating temperatures for the liquid-overfeed coils closely matched the manufacturer's literature values. The average brine temperatures were conservatively higher than the manufacturer's literature values. During discharge the tank outlet temperature held a constant value <35°F, as was expected from the manufacturer's data. Even when the system was deliberately overcharged, the cooling was available at only a slightly increased temperature.

The amount of capacity variation during a charge cycle, best shown by the normalized capacity plots, can have significant effects on the equipment performance and should be a primary factor in equipment selection. Because the amount of capacity variation is strongly related to charging rate, operating schedules must be an important consideration early in the system design.

Liquid-overfeed systems do require proper attention to oil return during design and installation. A minimum flow rate must be maintained through the refrigerant coils to assure no oil accumulation. Therefore, manufacturer's recommended refrigerant flow rates should be carefully followed. The oil return system, including the separator, still, and system bleed points, is a critical component of the system design.

REFERENCES

1. Baltimore Aircoil Company, *Ice Chiller Thermal Storage Units - for Thermal Storage Systems*, Bulletin S140/1-0C, Baltimore Aircoil Company, Baltimore, Md., 1985, amended by a September 14, 1987 Circular Letter from John M. McCullough to all BAC U.S. and Canadian Representatives; Subject: S140/1-0C, Ice Chiller Thermal Storage Units Glycol Pressure Drop Revisions.

2. T. K. Stovall and J. J. Tomlinson, *Commercial Cool Storage Laboratory Test Procedure*, ORNL/TM-11511, Martin Marietta Energy Systems, Inc., Oak Ridge Natl. Lab., May 1990.

3. P. V. Hobbs, *Ice Physics*, Clarendon Press, Oxford, 1974.

4. T. K. Stovall, *Ice-Storage Efficiency Considerations*, ORNL/TM-11678 (to be published).

5. G. T. Kartsounes and R. A. Erth, "Computer Calculation of the Thermodynamic Properties of Refrigerants 12, 22, and 502," *ASHRAE Transactions*, Vol. 77, Part 2, 1971.

6. *UCARTHERM Heat Transfer Fluid*, Union Carbide Corporation, Industrial Chemicals Division, Danbury, Conn., 1986.

7. *1986 ASHRAE Handbook, Refrigeration Systems and Applications*, American Society of Heating, Refrigerating and Air Conditioning Engineers, Inc., Atlanta, Ga., 1986, pp. 8.11–12.

8. *SAS User's Guide: Statistics*, Version 5 Ed., SAS Institute Inc., Cary, N.C., 1985.

9. *1985 ASHRAE Handbook, Fundamentals*, American Society of Heating, Refrigerating and Air Conditioning Engineers, Inc., Atlanta, Ga., 1985, Section 6.

10. *Commercial Cool Storage Design Guide*, EM-3981, Electric Power Research Institute, Palo Alto, Calif., May 1985.

Appendix A

ISTF INSTRUMENTATION

A.1 DATA ACQUISITION AND CONTROL

A data acquisition system and computer are used to control the thermal loading rate, the brine and refrigerant circulation pump speeds, recirculation valve positions, and the condensation temperature, and to collect the data from system instrumentation. The computer allows short sampling times of the instrumentation to provide data for detailed analysis and feedback during transient system operation. Direct controls, outside of the data acquisition/computer system, are available for compressor loading, booster pump operation, and auxiliary portions of the test facility.

A.2 TEMPERATURE MEASUREMENTS

Refrigerant temperature measurements are made by RTDs bonded to the outside of the copper pipes. These RTDs were calibrated by the manufacturer to 0.3°F. After installation, the recorded refrigerant temperatures were compared to the expected thermodynamic states for the corresponding pressure measurements. Water and brine temperature measurements are made by RTDs inserted into the PVC pipes. These RTDs are calibrated by the manufacturer to ± 0.5°F and are checked against an ice bath after installation. The RTDs were also checked against each other under conditions where an unloaded heat exchanger, for example, would be expected to show the same inlet and outlet temperature. The RTD calibrations are periodically rechecked, and instruments that have drifted beyond 0.5°F are replaced.

A.3 FLOW MEASUREMENTS

Vortex-shedding flowmeters are used to measure the condenser cooling water flow, the water/brine flow to the heater, the water/brine flow to the ice tank, and the gaseous refrigerant flow to the condenser. The vortex-shedding refrigerant flowmeter imposes a pressure drop of ~ 0.5 psia. These flowmeters are accurate to $\pm 0.8\%$ of the reading for liquid flows and $\pm 1.5\%$ of the reading for gaseous flows. The flowmeters used to measure

water and brine volumetric flow were checked after installation by running water through the lines into a 55-gal drum placed on a scale.

The Coriolis mass flowmeters used to measure liquid refrigerant mass flows to the low-pressure receiver, the ice tank, and the thermal expansion valves were calibrated by the manufacturer to $\pm 0.4\%$ of full scale, which is 1000 lb/min. A sight glass is positioned to provide a visual confirmation of single-phase flow downstream of the meter. These coriolis flowmeters are very difficult to calibrate after installation due to the closed nature of the refrigerant system. However, the volumetric flow through one of the vortex-shedding flowmeters can be compared to the mass flow through one of these Coriolis meters. Also, energy balances on the condenser, low-pressure receiver, chiller/evaporator, and ice tank can be used to assess the continued accuracy of these devices. Table A.1 summarizes many of these comparisons.

The closure balances reported in this table show that the measured refrigerant mass flows are consistently higher than those that would be calculated based on element balances against both brine and water measurements. For some tests, the flow rates appear to be somewhat accurate and for others seem to be off by a large amount. The differences between the two refrigerant flowmeters was tested against subcooling and the absolute flow rate. Significant correlations could be expected if FE1 was receiving liquid flow for some tests and a mixture of gas and liquid for tests with inadequate subcooling. The flow rate was also tested for correlations under the hypothesis that the flowmeter might be less accurate for some flow rates than others, although all flows were well within the bounds listed by the manufacturers. However, no correlations against either subcooling or flow rate could be found. Indeed, there are several examples of very similar test conditions where the flowmeter agreement is good for one test and poor for another. However, as the condenser energy balances show, the refrigerant volumetric flow rate from the vortex-shedding flowmeter is also suspect for some of the tests.

Air flow measurements for the agitation air supply are made by a rotometer with a calibrated accuracy of $\sim 0.6\%$.

Table A.1. Flowmeter/RTD comparative closure summary[a]

Test ID	Test type	Flowmeter comparison (FE5/VE1) ÷ FEI	Condenser balance: water capacity ÷ refrigerant capacity	Ice-tank balance: tank ice capacity ÷ brine capacity or tank ice capacity ÷ low-pressure receiver refrigerant capacity[a]	Chiller/ evaporator balance: brine capacity ÷ refrigerant capacity
0825	LO[b] discharge			1.0	
0913	LO discharge			1.2	
0915	LO discharge			1.0	
0524	B[c] discharge			1.0	
0608	B discharge			1.0	
0620	B discharge			1.1	
0626	B discharge			0.9	
0629	B discharge			1.0	
0707	B discharge			1.0	
0712	B charge			1.1	
0801	LO charge	1.3	0.6	0.6	
0811	LO charge	1.0	0.8	0.9	
0815	LO charge	1.1	0.6	0.7	
0824	LO charge	1.3	0.6	0.6	
0914	LO charge	1.0	0.8	0.9	
0922	LO charge	1.0	0.8	0.9	
0523	B charge	1.3	0.9	1.0	0.8
0613	B charge	1.2	0.9	1.0	0.8
0619	B charge	1.6	0.8	1.0	0.6
0623	B charge	1.6	0.8	1.0	0.6
0628	B charge	1.2	0.9	0.9	0.8
0727	B charge	1.1	0.9	1.2	0.9
0731	B charge	1.4	0.8	1.4	0.7
0803	B charge	1.1	0.9	1.2	0.9

[a]Refrigerant capacity based on FE5.
[b]LO = liquid-overfeed coils.
[c]B = brine coils.

A.4 PRESSURE MEASUREMENTS

Refrigerant pressure measurements are made with pressure transducers to allow the electronic recording of the values. The accuracy of these absolute pressure readings is rated at ±0.11% of full scale. However, the calibration certificates supplied with each transducer show accuracies of ±0.004% or better. Also, the transducer calibration was rechecked after

installation and periodically thereafter using laboratory calibration equipment. The pressure transducers located in the high-pressure portion of the loop, that is, between the compressor discharge and the expansion valve, are rated for 0 to 500 psia. All others are rated for 0 to 250 psia. During testing, the pressure measurements are periodically compared to other measurements within the loop and to the expected refrigerant properties.

A differential pressure meter can be used to measure the change in tank water depth during charging. The meter measures from 0 to 10 in. of water with an accuracy of $\pm 0.5\%$ of full-range output (i.e., ± 0.05 in. of water).

A.5 ELECTRICAL MEASUREMENTS

Electrical measurements for the compressor power (rated at 40 and 75 hp), circulating pump(s) power (from 2 to 5 hp), agitation air compressor power (1/2 hp), and heater power (0 to 135 kW) are measured by watt/watt-hour transducers. The watt-hour measurements are accurate to $\pm$[0.2% of the reading + 0.01% of the rated output)/(power factor)]. The watt-hour meters for the compressors were checked by measuring the voltage and current on each of three phases. The watt-hour meter for the heater was checked by comparison to the heat absorbed by the water as measured by the flow and temperature change. The accuracy of this heater's watt-hour meter is poor because of the semiconduction controlled rectifier (SCR), used to vary the heater power. Heater energy use measurements are therefore based on the fluid flow rate and temperature change, although the power consumption is recorded as an additional check.

A.6 COOL STORED MEASUREMENT

The change in storage medium volume is used to measure the amount of expansion due to ice formation on coil systems. The amount of ice formation and the sensible heat removed from the storage medium indicate the quantity of cool stored in the tank.

A standpipe was attached to the storage tank, and the differential pressure transducer described in a previous section was mounted at BAC's recommended initial water level. This arrangement permits the data recording system to continuously record the tank water height.

Appendix B

BAC COMPUTER SIMULATION

BAC uses a detailed computer code to aid in selecting the proper ice storage model for individual applications. Typically, the customer will provide the amount of ice storage needed and two compressor operating points (from a compressor curve) near the anticipated chiller temperature (based on BAC catalogue data). Pressure drops between the chiller outlet and the compressor suction must be added because the code is based on conditions at the chiller. The BAC code then calculates the predicted chiller temperature and compressor capacity for the proposed storage system. These two values are calculated simultaneously for each time step, based on the capacity, temperature, and ice thickness values during the previous time step (assuming a linear compressor capacity curve between the two given values). The time-weighted average chiller temperature and compressor capacity during the ice build are then calculated and reported to the customer.

For comparison to the test data, the measured capacity (corrected for the liquid-overfeed coils and uncorrected for the brine coils) was used in place of the compressor model. The standby and agitation losses were added to the capacity, because the code is based on coil capacity, and these losses will be application-specific. The code's chiller model was then used with this capacity to predict the chiller temperature throughout the ice-building cycle. The predicted chiller temperature is compared to the measured chiller temperature in Tables B.1 and B.2 and Figs. B.1–B.13. (These figures include data from early test portions that were deleted from the analysis presented elsewhere in this report.) The computer code is only applicable during the ice-build time. Therefore, cooldown data were eliminated from the comparison. For the liquid-overfeed tests, these figures also show the saturated temperature corresponding to the chiller outlet pressure. The difference between the measured and predicted liquid-overfeed average coil outlet temperatures range from −0.2 to +0.9°F, and average +0.3°F. The difference between the average saturated temperatures corresponding to the measured pressures leaving the liquid-overfeed coils and the predicted values range from +0.8 to +2.0°F and average +1.4°F. The difference between measured temperatures entering the brine coils and the predicted values (based on the uncorrected capacity measurements) range from −1.2 to +0.9°F and average −0.3°F. The difference between the measured temperatures and the predicted values (based on corrected capacity measurements

Table B.1. BAC computer simulation liquid-overfeed coil temperatures

Test ID	Average capacity[a] (tons)	Average corrected capacity[b] (tons)	Average suction temperature (°F)			
			Measured	Saturated	Predicted	Predicted[c]
0801	14.2	14.6	25.5	26.5	25.7	25.5
0811	39.6	42.0	16.4	16.4	15.4	14.2
0815	20.9	21.4	24.1	24.1	22.7	22.4
0914	38.3	39.8	17.9	17.9	16.1	15.4
0922	38.4	40.8	18.0	18.0	16.0	14.8

[a]Corrected according to change in tank height.

[b]Corrected according to change in tank height with ice density modifications.

[c]Predicted with ice density modifications to compressor capacity.
Source: Tom Carter, Baltimore Aircoil Company.

Table B.2. BAC computer simulation brine-coil temperatures

Test ID	Average capacity[a] (tons)	Average corrected capacity[b] (tons)	Average tank inlet temperature (°F)		
			Measured	Predicted	Predicted[c]
0523	23.7	24.5	16.6	16.5	16.1
0613	22.4	22.8	18.1	17.9	17.7
0619	14.0	14.7	23.1	23.3	23.0
0623	13.5	14.8	23.4	23.5	23.0
0628	22.7	21.7	18.4	17.5	18.1
0727	25.6	32.8	18.8	20.0	16.9
0731	11.4	17.1	25.4	26.6	24.6
0803	21.6	26.6	21.2	21.8	19.8

[a]Based on brine flow rate and temperature change, uncorrected.

[b]Corrected according to change in tank height with ice density modifications.

[c]Predicted with ice density modifications to compressor capacity.
Source: Tom Carter, Baltimore Ancoil Company.

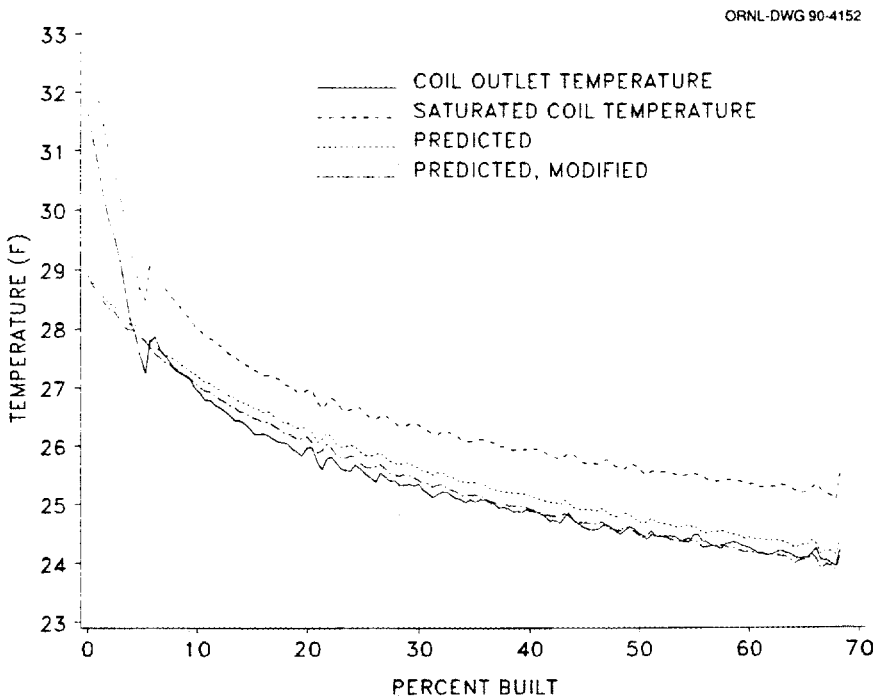

Fig. B.1. Comparison of test data to BAC computer model predictions for liquid-overfeed test of 0801. All temperature measurements are ±0.5°F.

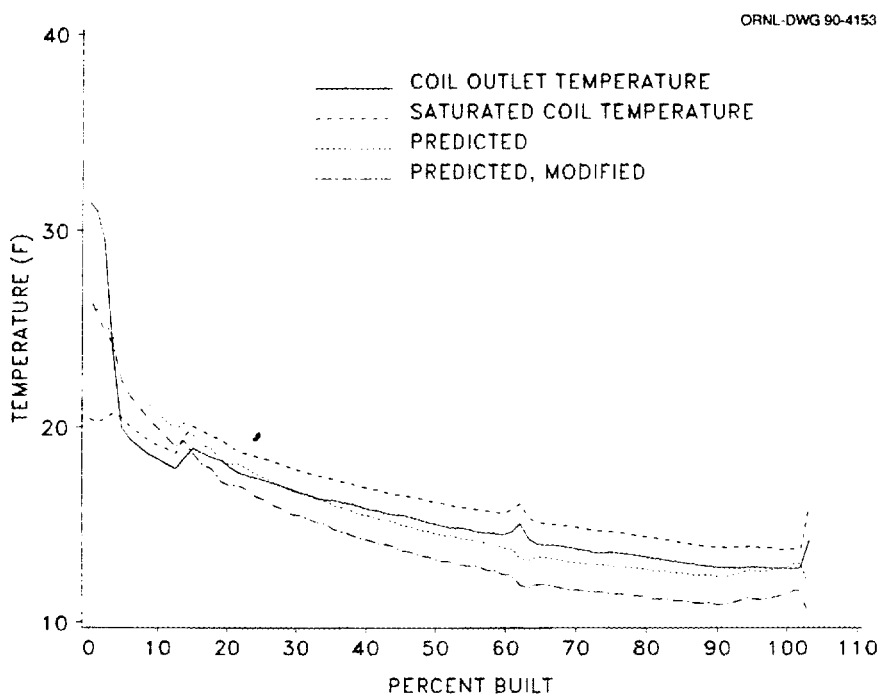

Fig. B.2. Comparison of test data to BAC computer model predictions for liquid-overfeed test of 0811. All temperature measurements are ±0.5°F.

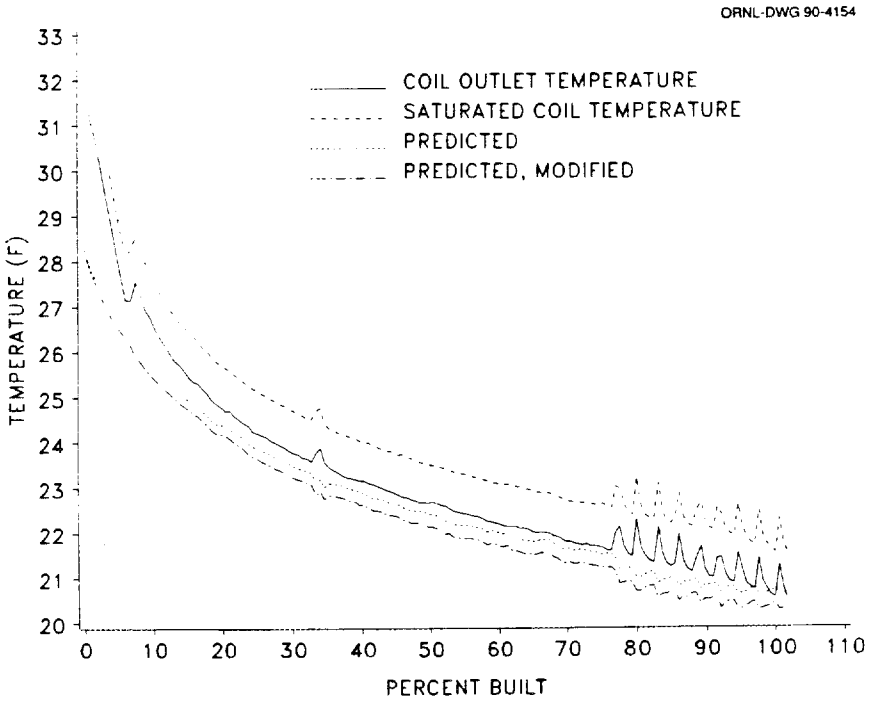

Fig. B.3. Comparison of test data to BAC computer model predictions for liquid-overfeed test of 0815. All temperature measurements are ±0.5°F.

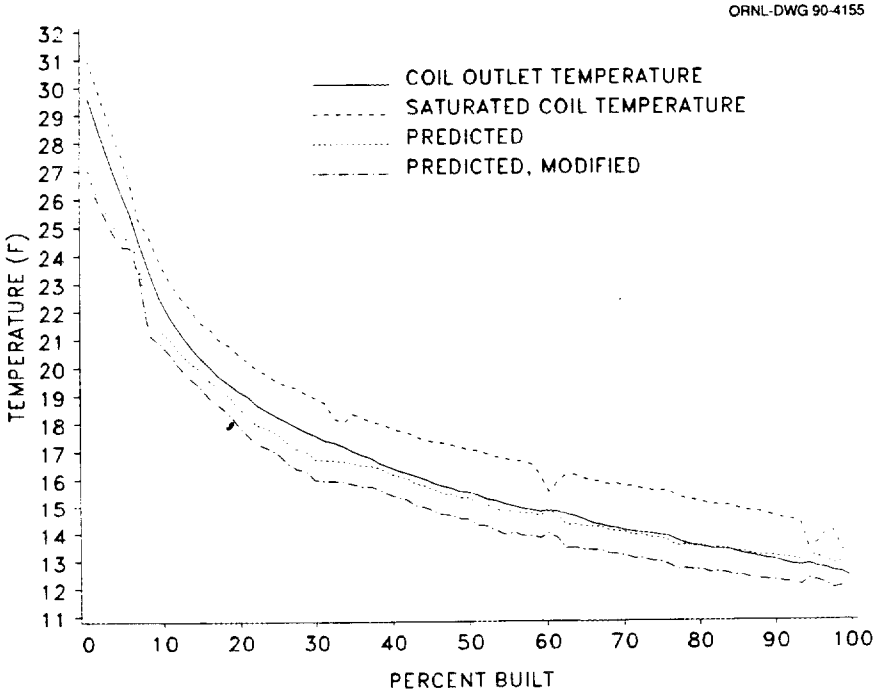

Fig. B.4. Comparison of test data to BAC computer model predictions for liquid-overfeed test of 0914. All temperature measurements are ±0.5°F.

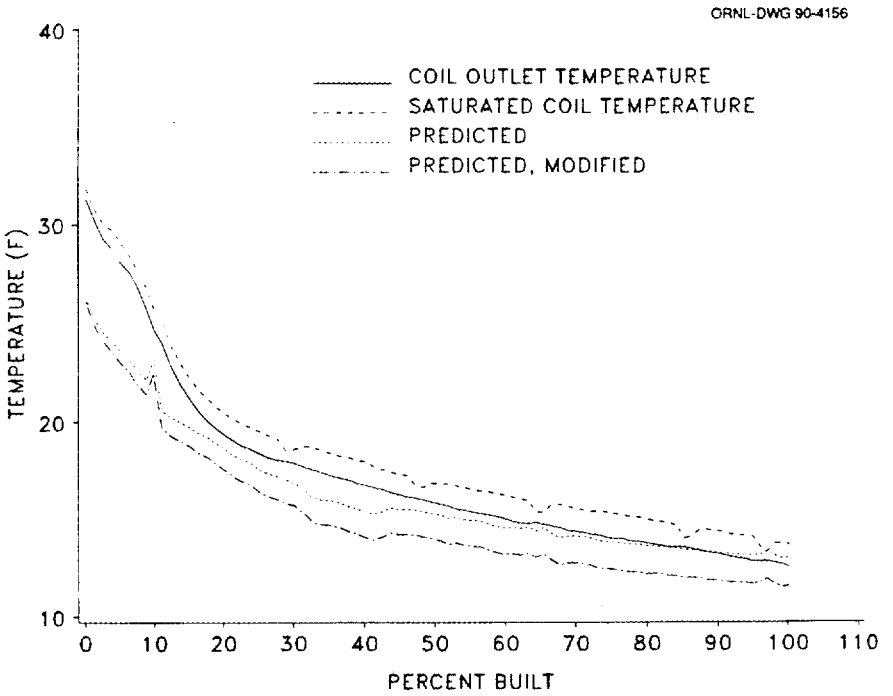

Fig. B.5. Comparison of test data to BAC computer model predictions for liquid-overfeed test of 0922. All temperature measurements are ±0.5°F.

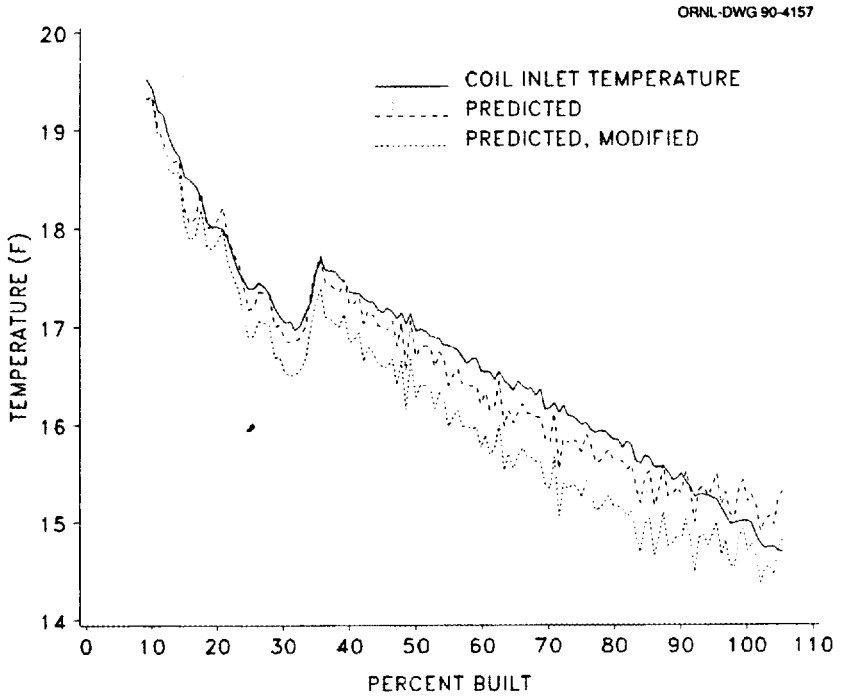

Fig. B.6. Comparison of test data to BAC computer model predictions for brine-coil test of 0523. All temperature measurements are ±0.5°F.

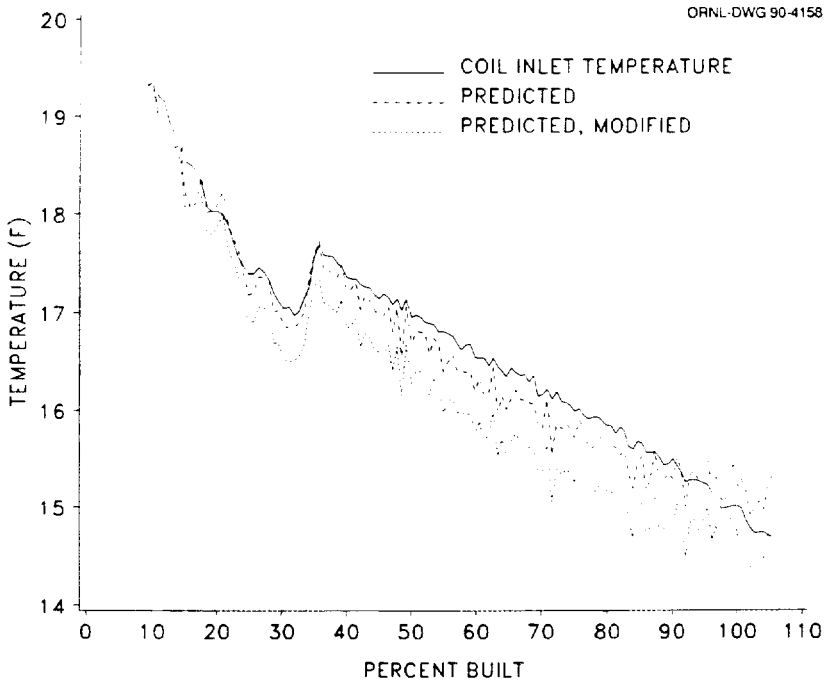

Fig. B.7. Comparison of test data to BAC computer model predictions for brine-coil test of 0613. All temperature measurements are ±0.5°F.

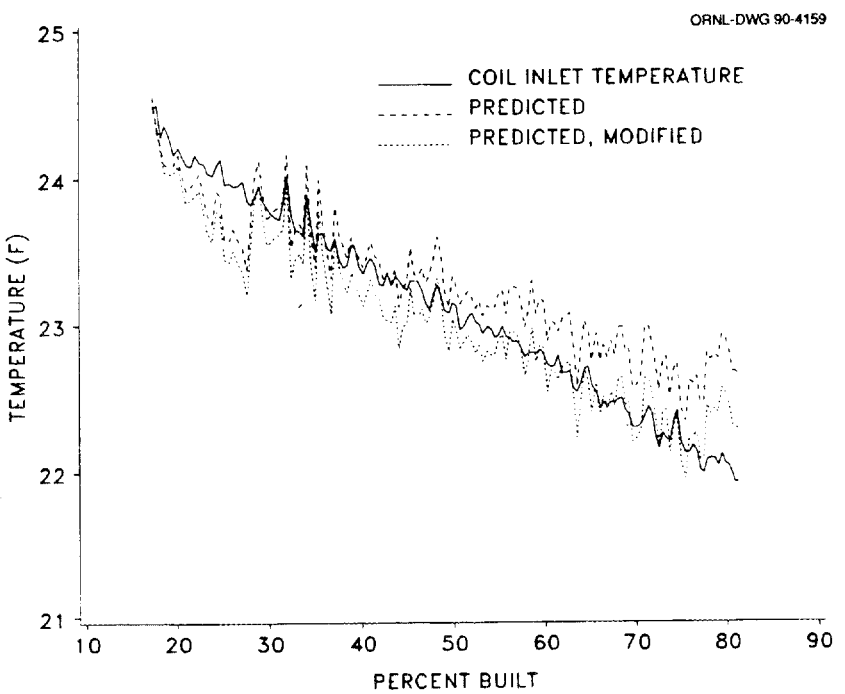

Fig. B.8. Comparison of test data to BAC computer model predictions for brine-coil test of 0619. All temperature measurements are ±0.5°F.

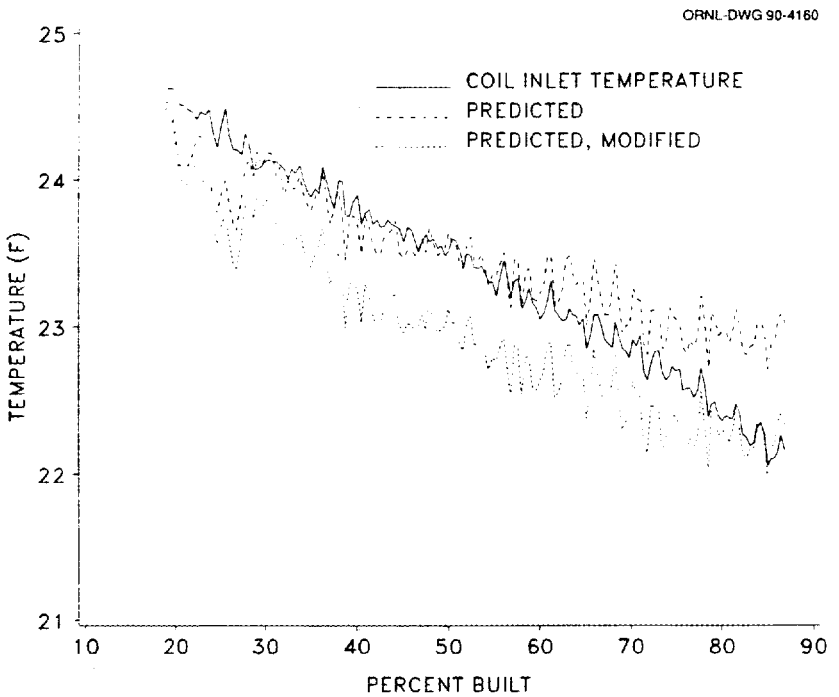

Fig. B.9. Comparison of test data to BAC computer model predictions for brine-coil test of 0623. All temperature measurements are ±0.5°F.

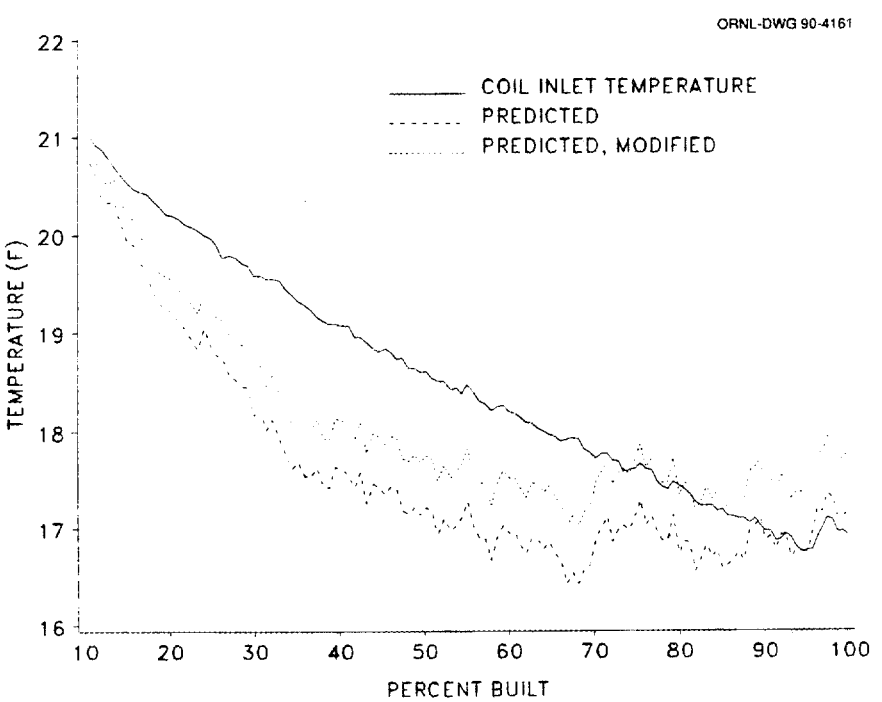

Fig. B.10. Comparison of test data to BAC computer model predictions for brine-coil test of 0628. All temperature measurements are ±0.5°F.

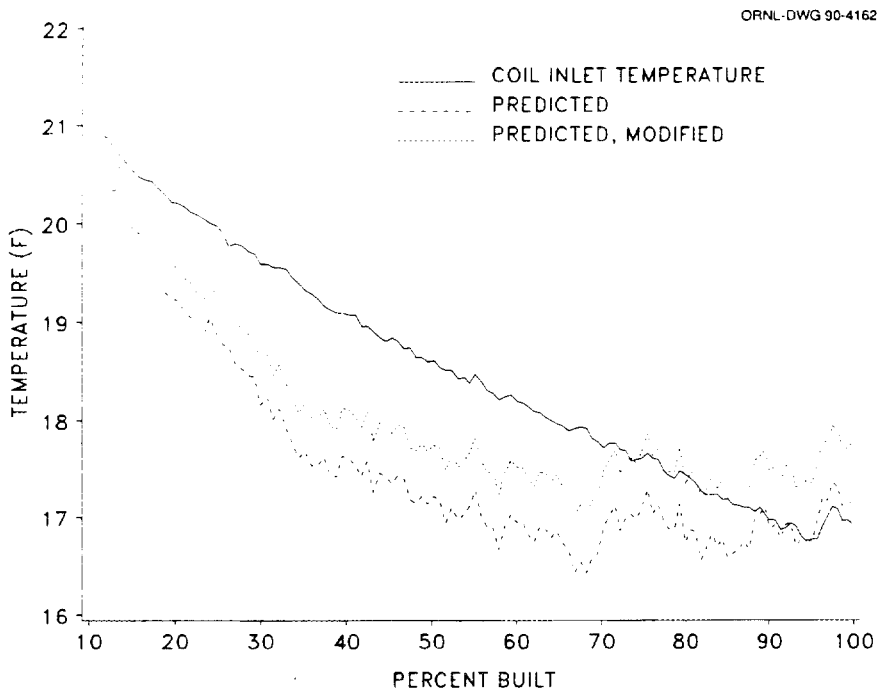

Fig. B.11. Comparison of test data to BAC computer model predictions for brine-coil test of 0727. All temperature measurements are ±0.5°F.

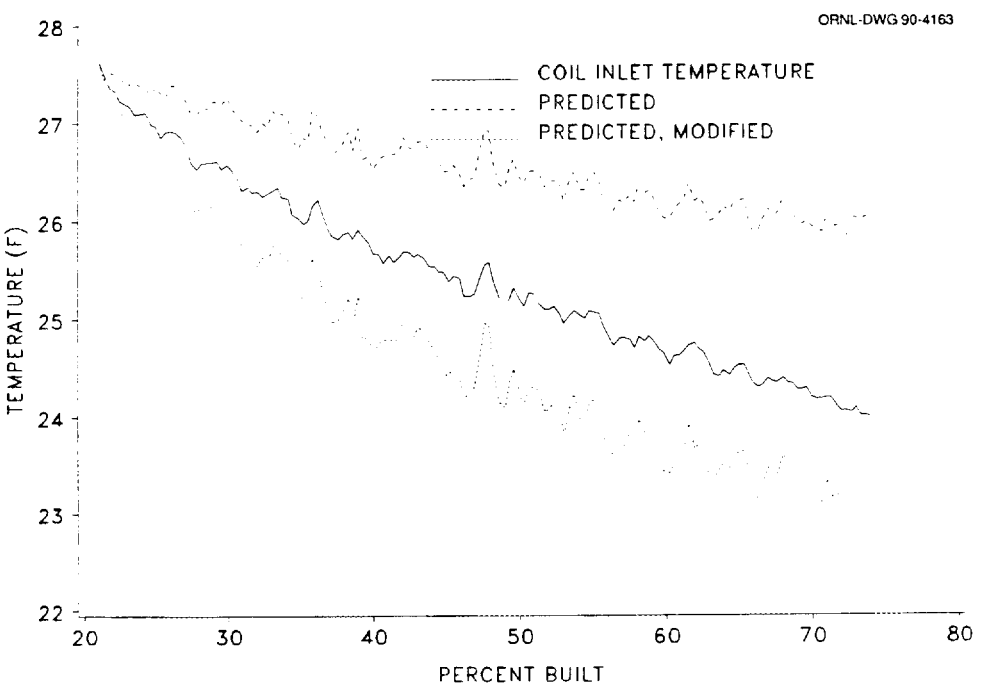

Fig. B.12. Comparison of test data to BAC computer model predictions for brine-coil test of 0731. All temperature measurements are ±0.5°F.

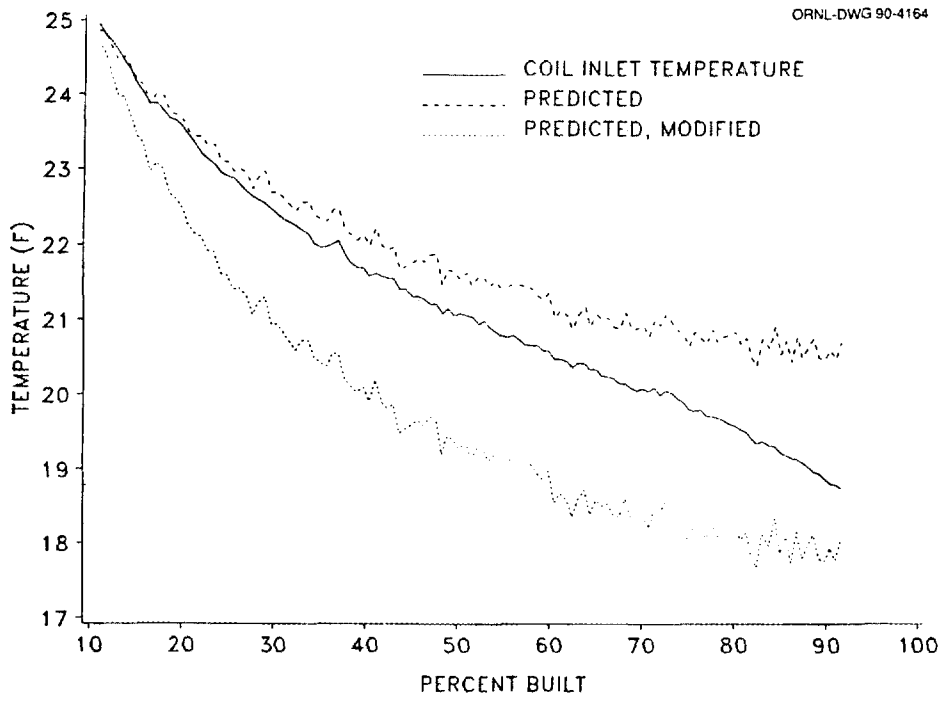

Fig. B.13. Comparison of test data to BAC computer model predictions for brine-coil test of 0803. All temperature measurements are ±0.5°F.

using an assumed ice density of 57.3 lb/ft^3) entering the brine coils ranged from +0.1 to +1.9°F and average +0.7°F. A positive difference is conservative; that is, the measured temperature is higher than the predicted temperature.

BAC uses a standard ice density value of 57.3 lb/ft^3. As mentioned in the earlier text, the experimental value used in converting changes in tank height to capacity was 57.2 lb/ft^3. To show the importance of this number, BAC corrected the experimental capacity values to reflect the capacity that would be measured if an ice density value of 57.3 lb/ft^3 were used to convert measured changes in water height to ton-hour of ice stored. The range of differences between the saturated temperature and the predicted temperature would then be from +0.2 to +3.2. These numbers show a higher degree of conservatism and are also shown in Table B.1.

ORNL/TM-11342
Dist. Category UC-202

Internal Distribution

1. T. D. Anderson
2. V. D. Baxter
3. S. H. Buechler
4. R. S. Carlsmith
5. W. G. Craddick
6. P. D. Fairchild
7. D. J. Fraysier
8. W. Fulkerson
9. R. B. Honea
10. J. E. Jones Jr.
11. L. Jung
12. R. J. Kedl
13. M. A. Kuliasha
14. W. A. Miller
15. W. R. Mixon
16. M. Olszewski
17. A. E. Ruggles
18. A. C. Schaffhauser
19. M. Siman-Tov
20-29. T. K. Stovall
30. J. J. Tomlinson
31. C. D. West
32. G. L. Yoder
33. ORNL Patent Section
34. Central Research Library
35. Document Reference Section
36-37. Laboratory Records Department
38. Laboratory Records (RC)

External Distribution

39. John Stephen Anderpont, Chigago Bridge & Iron Company, 800 Jorie Boulevard, Oak Brook, IL 60522-7001
40. Debra L. Catanese, P.E., Pennsylvania Electric Company, 311 Industrial Park Rd., Johnstown, PA 15904
41. Tom Carter, Baltimore Aircoil Company, P.O. Box 7322, Baltimore, MD 21227
42. Russ Eaton, Director, Advanced Utility Concepts Division, U.S. Department of Energy, Forrestal Building, CE-142, 1000 Independence Avenue, Washington, DC 20585
43. Imre Gyuk, Office of Energy Storage and Distribution, U.S. Department of Energy, Forrestal Building, CE-32, 1000 Independence Avenue, Washington, DC 20585
44. Landis Kannberg, Battelle Pacific Northwest Laboratories, P.O. Box 999, Battelle Boulevard, Richland, WA 99352
45. Don Kemp, Turbo Refrigerating Company, 1815 Shady Oaks Drive, P.O. Box 396, Denton, TX 76202
46. K. W. Klunder, Director, Office of Energy Management, Department of Energy, CE-14, Forrestal Building, 1000 Independence Avenue, Washington, DC 20585
47. Dave Knebel, Paul Mueller Company, P.O. Box 828, Springfield, MO 65801-0828
48. David Laybourn, P.E., Director of Marketing, Reaction Thermal Systems, Inc., 840 Latour Court, Suite A, Napa, CA 94558
49. George Manthey, DOE, Oak Ridge Operations, Oak Ridge, TN 37831
50. Robert P. Miller, Baltimore Aircoil Company, P.O. Box 7322, Baltimore, MD 21227

52. Dave Pellish, U.S. Department of Energy, Forrestal Building, MS CE-332, Room 5H-79, 100 Independence Avenue, Washington, DC 20585
53. Veronika A. Rabl, Electric Power Research Institute, 3412 Hillview Avenue, P.O. Box 10412, Palo Alto, CA 94303
54. Eberhart Reimers, Advanced Utility Concepts Division, U.S. Department of Energy, Forrestal Building, CE-142, 1000 Independence Avenue, Washington, DC 20585
55. Richard Rhodes, FAFCO, Inc., 235 Constitution Drive, Menlo Park, CA 94025
56. Marwan Saliba, Energy Engineering Institute, Dept. of Mechanical Engineering, San Diego State University, San Diego, CA 92182-0191
57. Brian Silvetti, Calamac Manufacturing Corporation, Box 710, 150 South Van Brunt Street, Englewood, NJ 07631
58. Robert L. San Martin, Deputy Assistant Secretary, Office of Utility Technology, Department of Energy, CE-10, 6C-026/Forrestal Bldg., 1000 Independence Avenue, Washington, DC 20585
59. Chang W. Sohn, U.S. Army Corps of Engineers, P.O. Box 4005, Champaign, IL 61824-4005
60. Laura Thomas, Marketing Manager, York International Corporation, P.O. Box 1592, York, PA 17405-1592
61. Samuel G. Tornabene, Edison Electric Institute, 1111 19th Street, N.W., Washington, DC 20036-3691

62-71. R. D. Wendland, Electric Power Research Institute, 3412 Hillview Avenue, Box 10412, Palo Alto, CA 94303

72. Maurice W. Wildin, Professor, The University of New Mexico, Department of Mechanical Engineering, Albuquerque, NM 87131
73. Office of Assistant Manager for Energy Research and Development, Department of Energy, ORO, Oak Ridge, TN 37831

74-85. Given distribution as shown in DOE/OSTI-4500-R75 under Category UC-202 (Thermal Energy Storage)